2016-01-01

Mechanically Activated Combustion SynThesis Of Molybdenum Borosilicides For Ultrahigh-Temperature Structural Applications

Alan Alberto Esparza Hernandez
University of Texas at El Paso, aaesparza3@miners.utep.edu

MECHANICALLY ACTIVATED COMBUSTION SYNTHESIS OF MOLYBDENUM BOROSILICIDES FOR ULTRAHIGH-TEMPERATURE STRUCTURAL APPLICATIONS

ALAN A. ESPARZA HERNANDEZ

Master's Program in Mechanical Engineering

APPROVED:

Evgeny Shafirovich, Ph.D., Chair

Yirong Lin, Ph.D.

David A. Roberson, Ph.D.

Charles Ambler, Ph.D.

Dean of the Graduate School

DEDICATION

To my parents and brother, thank you for raising the bar.

COMBUSTION SYNTHESIS OF MECHANICALLY ACTIVATED MOLYBDENUM BOROSILICIDES FOR ULTRAHIGH-TEMPERATURE APPLICATIONS

by

ALAN A. ESPARZA HERNANDEZ

THESIS

Presented to the Faculty of the Graduate School of

The University of Texas at El Paso

in Partial Fulfillment

of the Requirements

for the Degree of

MASTER OF SCIENCE

Department of Mechanical Engineering

THE UNIVERSITY OF TEXAS AT EL PASO

May 2016

Acknowledgements

I would like to extend my most sincere gratitude to my advisor and mentor Dr. Evgeny Shafirovich. I will need to write another 70 pages to fully thank him for his guidance and advice.

Also, my committee members, Dr. Yirong Lin and Dr. David Roberson.

I would like to thank my colleagues, especially Armando Delgado and Mohammad Alam for their guidance, Sergio Guerrero, Sergio Cordova, and Arturo Catalan.

I would like to thank Alma Leaños and Alejandra Cabral, and Ricardo Martinez for their assistance in the preparation of my samples, and nano indentation tests, respectively.

This material is based upon work supported by the Department of Energy under Award Number DE-FE0008470. This work was also supported by Climax Molybdenum, Inc.

Abstract

The thermal efficiency of gas-turbine power plants could be dramatically increased by the development of new structural materials based on molybdenum silicides and borosilicides, which can operate at temperatures higher than 1300 °C with no need for cooling. A major challenge in their development is to simultaneously achieve high oxidation resistance and acceptable mechanical properties at elevated temperatures. Materials based on Mo_5SiB_2 (called T_2) phase offer favorable combinations of high-temperature mechanical properties and oxidation resistance. Multi-phase (e.g., α-Mo–Mo_5SiB_2–Mo_3Si and Mo_5SiB_2–TiC) alloys have been proposed for this purpose. However, the synthesis of Mo-Si-B multi-phase alloys is usually difficult because of their extremely high melting points. In the present work, a combustion route has been explored to fabricate these materials. Specifically, the use of mechanically activated self-propagating high-temperature synthesis (MASHS) has allowed us to obtain, for the first time, materials based on T_2 phase and titanium diboride (TiB_2), but initially they included unwanted secondary phases. To overcome this problem, the so-called "chemical oven" technique has been implemented, which has enabled combustion synthesis of Mo_5SiB_2−TiB_2, Mo_5SiB_2–TiC, and α-Mo–Mo_5SiB_2–Mo_3Si materials. Oxidation tests have shown that, among them, Mo_5SiB_2–TiB_2 material exhibits the best oxidation resistance at high temperatures. Studies of mechanical properties have shown that Mo_5SiB_2–TiB_2 material also has the highest elastic modulus and hardness at room temperature among the materials tested.

Table of Contents

Table of Figures

Chapter 1: Introduction

1.1 Project Rationale

1.1.1 Advantages and problems of molybdenum silicides as structural materials for ultrahigh-temperature applications

The desire to improve the efficiency of gas-turbine power plants has led to a relentless quest for new, ultrahigh-temperature structural materials to replace the current nickel-based superalloys. These materials have reached the maximum allowable operating temperature determined by the melting temperature of these alloys, which is about 1150 °C. Cooling systems as well as thermal barrier coatings (TBC) have been developed to push the thermal boundaries of these materials. However, the addition of an external cooling system significantly lessens the overall engine performance. Although the use of thermal barrier coatings is a viable alternative, there are risks of catastrophic and complex failures such as thermal stresses, the oxidation of the metal, and the constant changing in the microstructure and properties of the TBC system [1].

The development of new structural materials with higher melting temperatures than nickel-based superalloys is an attractive alternative for increasing the thermal efficiency of power plants. One of these materials is $MoSi_2$, which has been widely recognized as a promising option for high-temperature applications because of its high melting point, 2030 °C, exceptional oxidation resistance, and reasonable density, 6.24 g/cm^3. $MoSi_2$ was first discovered in 1907 and was labeled as a high-temperature corrosion resistant coating material [2]. $MoSi_2$ can be used at temperatures above 1100 °C without oxidation limiting its performance [3]. However, $MoSi_2$ is not a suitable material for structural applications because of its poor mechanical properties. Brittleness at room temperature leads to low fracture toughness, while poor creep rates are exhibited in elevated temperatures. For this reason, other materials should be investigated such as molybdenum silicides and borosilicides [4, 5, 6, 7].

Mo-rich silicides are also attractive owing to their good mechanical properties. For example, Mo_5Si_3 has an elastic modulus of 323 GPa and a melting point of 2180 °C [8]. However,

Mo_5Si_3 exhibits poor oxidation resistance at elevated temperatures [9, 10]. Summarizing, the addition of Mo improves mechanical properties but decreases the oxidation resistance.

1.1.2 The addition of boron to molybdenum borosilicides

One promising solution is the addition of boron, which improves the oxidation resistance of molybdenum silicides [11], while high concentrations of Mo phase improve the ductility and fracture toughness of these materials [12]. This has promoted interest in fabricating boron-added Mo-rich silicides such as Mo_5SiB_2 (T_2) phase and α-Mo–Mo_5SiB_2–Mo_3Si. These materials combine good oxidation resistance and acceptable mechanical properties [12, 13, 14].

Further, a novel method for improving the mechanical properties of Mo_5SiB_2 materials involves the addition of titanium carbide (TiC), which has a melting point of 2887 °C and a modulus of elasticity of 379 GPa at 1000 °C [15]. Recently, it has been shown that TiC improves the mechanical properties of the main Mo-Si-B network [16, 17].

Another potential option to strengthen T_2-based materials is the addition of titanium diboride (TiB_2), which has a melting point of 3230 °C and an elastic modulus of 534 GPa at 1000 °C [18]. However, to the best of our knowledge, the phase diagram for TiB_2 and Mo-Si-B phases is not available and no attempt has been made to fabricate Mo_5SiB_2–TiB_2 materials.

1.1.3 Synthesis of molybdenum borosilicides

Generally, it is difficult to synthesize Mo-Si-B alloys due to their extremely melting temperatures. Mechanical alloying has been used to fabricate these materials, but it required long milling times (typically 10-100 h), leading to large energy consumption and contamination of the products by the grinding media [14, 19].

It would be attractive to use self-propagating high-temperature synthesis (SHS) for the fabrication of T_2 phase based alloys because of its higher energy efficiency and better purification capability than the conventional fabrication techniques [20]. A major problem, however, is low

exothermicities of mixtures for producing these materials. One promising method for enabling the SHS process in low-exothermic mixtures is mechanical activation of the powders, i.e. a short-duration, high-energy ball milling step before the combustion process [21, 22]. The entire procedure is usually called mechanical activation-assisted (or mechanically activated) self-propagating high-temperature synthesis (MASHS). The high-energy milling enables intermixing of reactive components on a very small scale. The fracture-welding process during milling increases the contact surface area and destroys the oxide layer on the particle surface. As a result, mechanical activation improves the reaction kinetics, leading to an easier ignition and stable combustion. Also, the short milling time eliminates the problem of product contamination by milling media, typical for mechanical alloying. In general, the MASHS technique combines the advantages of mechanical alloying and SHS, also allowing for the formation of materials that cannot be obtained by either of these techniques if used alone.

Sometimes, however, the use of mechanical activation is insufficient for ignition. In such cases, the exothermicity can be increased by changing the mixture ratio. Another method, for example, is the so-called "chemical oven," where the sample is surrounded by a layer of a highly exothermic mixture such as Ti/C or Ti/B. Combustion of this layer releases enough heat for enabling ignition and combustion of the core material. Recently, this method has been successfully employed for the fabrication of T_2 phase [23].

1.2 Objectives

The research goals of this study include the development of structural materials based on Mo_5SiB_2 for ultrahigh temperature applications and the implementation of combustion-based route for fabricating these materials. Specifically, this project investigates:

- The feasibility of fabricating materials based on Mo_5SiB_2 and TiC using the mechanical activated self-propagating high temperature synthesis (MASHS) and the "chemical oven" combustion synthesis technique.

- The feasibility of fabricating materials based on Mo_5SiB_2 and TiB_2 using MASHS and the chemical oven technique.
- The feasibility of fabricating α-Mo–Mo_5SiB_2–Mo_3Si materials using MASHS and the chemical oven technique
- The oxidation properties of the materials fabricated by MASHS and the chemical oven technique.
- The mechanical properties of the materials fabricated by the chemical oven technique.

Chapter 2: Literature Review on Molybdenum Borosilicides for Ultrahigh-Temperature Applications

2.1 Oxidation resistance of Mo-Si-B materials

$MoSi_2$ and Mo_5Si_3 were considered a viable option to replace Ni-based superalloys. The former has an exceptional oxidation resistance due the formation of SiO_2, but there is no feasible way $MoSi_2$ can mechanically perform [3, 24]. On the other hand, Mo_5Si_3 has very good mechanical properties, suitable for structural applications, but exhibits lower oxidation resistance [9, 10]. To solve this problem, the addition of secondary phases to molybdenum silicides has been extensively studied.

It has been demonstrated that the addition of boron to molybdenum silicides greatly improves their oxidation resistance. Meyer et al. found that small additions as 0.14 wt% of boron greatly increases the oxidation resistance of Mo_5Si_3 at 1450 °C because of the formation of a protective borosilicate glass. The products contained Mo_5Si_3, Mo_5SiB_2 (T_2), Mo_3Si, $MoSi_2$, and MoB [25].

The formation of the borosilicate protective layer was subject of further study. Meyer et al. found that this glass layer starts to form at temperatures around 600 °C. However, at those temperatures the oxidation of Mo is faster than the formation of the borosilicate layer and rapid mass loss is exhibited at 750 °C. This mass loss is attributed to the volatilization of MoO_3 [26].

Furthermore, Akinc et al. studied the isothermal oxidation of Mo_5si_3 and B-Mo_5Si_3. These materials exhibited an initial weight loss, but it was directly dependent on the molybdenum content and the B/Si ratio. At higher B+Si contents, this initial loss is reduced. Also, undoped Mo_5Si_3 had the worst oxidation resistance [27].

Ito et al. found that the oxidation rate varied inversely with the ratio of B/Si in the Mo-Si-B network. They significantly enhanced the oxidation resistance by increasing the B/Si content through using Mo-9Si-18B composition. They showed that Mo-Si-B alloys are susceptible to rapid oxidation at temperatures between 600 and 750 °C. Nevertheless, oxidation is reduced at temperatures above 1000 °C because of the formation of the borosilicate layer. Mass gains less than 1 mg/cm^2 at 1300 °C and up to 2 mg/cm^2 at 1500 °C were reported [28].

In addition, Kruger et al. found that highest concentrations of Si and B deliver the highest oxidation resistance. As seen in Figure 2.1.1, the least oxidation-resistant material contained the lowest concentration of Si+B [29].

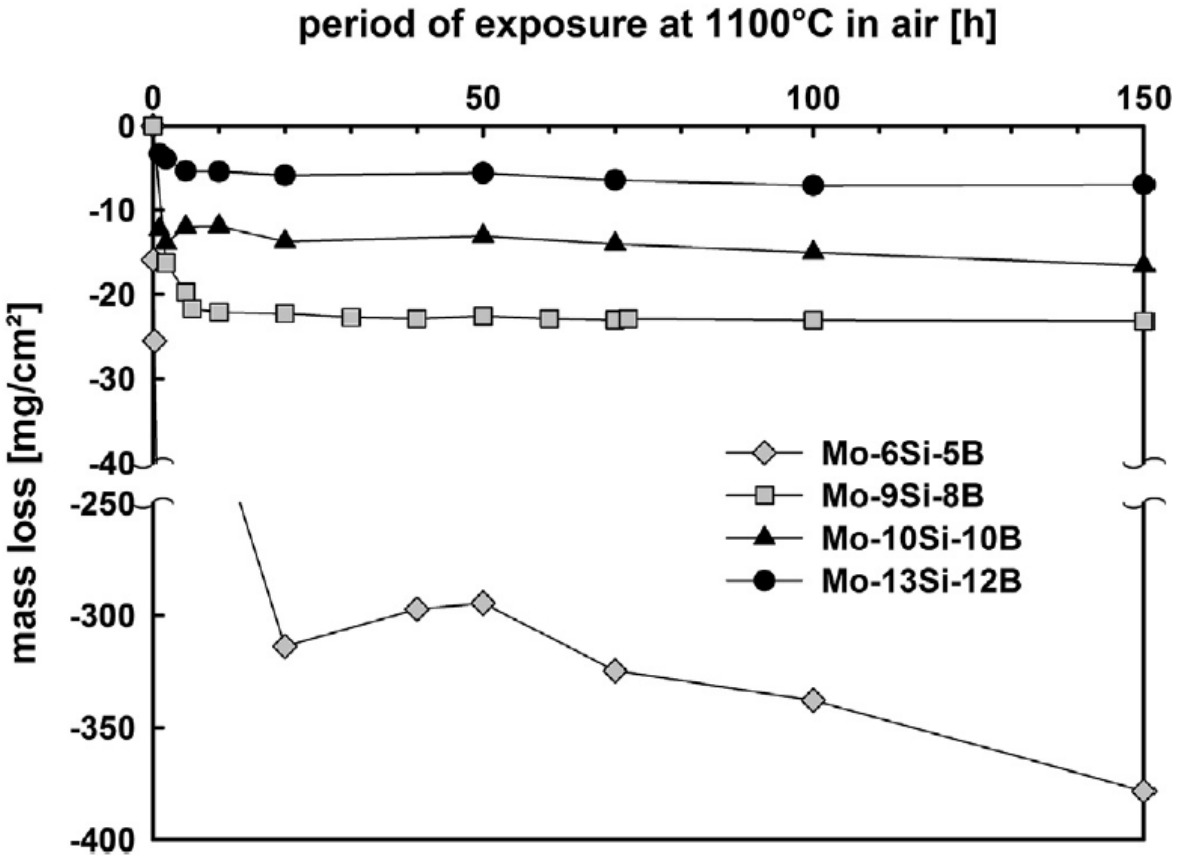

Figure 2.1.1: Oxidation behavior of different Mo-Si-B alloys at 1100 °C in air [29].

Likewise, Choe et al. found that the formation effect of the protective layer is negligible at temperatures below 600 °C, while the largest mass loss is at 800 °C. However, the oxidation rate is decreased at 800 °C thanks to the formation of B_2O_3/SiO_2 and the weight loss was almost stopped at 900 °C [30].

Similarly, Mendiratta et al. found that the protective layer cannot be formed at temperatures below 800 °C because volatilization of MoO_3 drives the oxidation. However, the protection is provided at temperatures between 1000 and 1300 °C [31].

Schneibel et al. experimented with different Mo concentrations in the α-Mo-Mo_3Si-Mo_5SiB_2 alloy and found that higher molybdenum content led to faster oxidation. In addition, they stated that the Mo volume fraction should be smaller than 50 vol% in order to obtain acceptable oxidation resistance [32].

Mandal et al. studied the oxidation behavior of α-Mo-Mo_3Si-Mo_5SiB_2 materials in wet air. Again, it was found that the higher concentrations of Mo were directly related to poor oxidation resistance. Also, they identified that water vapor accelerated the growth of the protective borosilicate glass and α-Mo-Mo_3Si-Mo_5SiB_2 materials were particularly sensitive to water accelerated growth [33].

In the same way, Wang et al. studied the Mo-12.5Si-25B and Mo-14Si-28B (at%) compositions. They found that even when the B/Si ratio remained constant, the alloy with the higher boron content provided the better oxidation resistance [34].

Yoshimi et al. were able to characterize the oxide layer found in a Mo-MoB-Mo_5Si_3-Mo_5SiB_2 alloy. In Figure 2.1.2, it is seen that Mo was present in the oxide layer, while MoO_2 was trapped in an intermediate layer between the protective glass and the substrate [35].

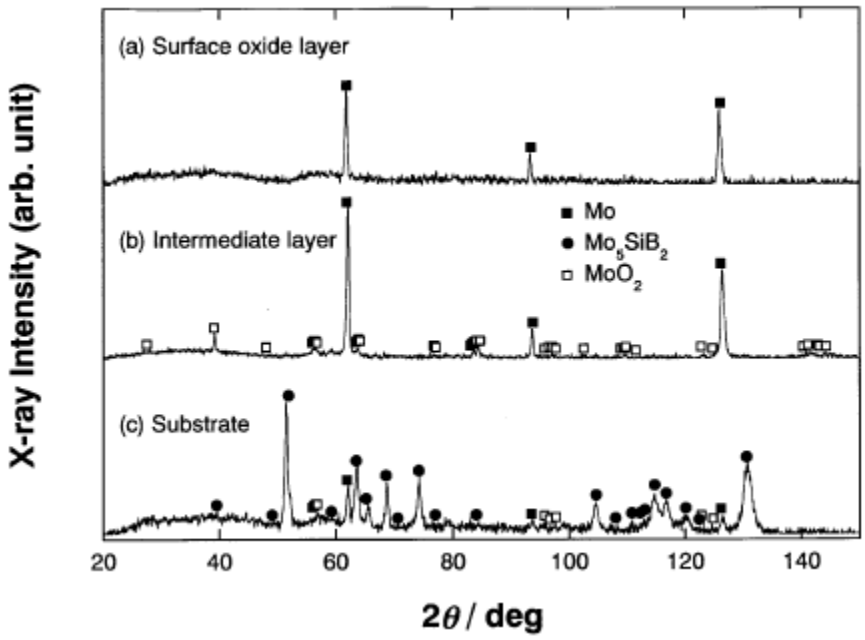

Figure 2.1.2: Micro-area XRD profiles obtained from (a) top layer, (b) interlayer and (c) substrate [35].

Dimiduk et al. summarized in Figure 2.1.3 that boron addition slow the oxidation process. Also, at temperatures lower than 800 °C and low concentrations of B, the oxidation by MoO_3 volatilization is significantly fast. For this reason, Mo-Si-B alloys should operate at temperatures above 1000 °C [36].

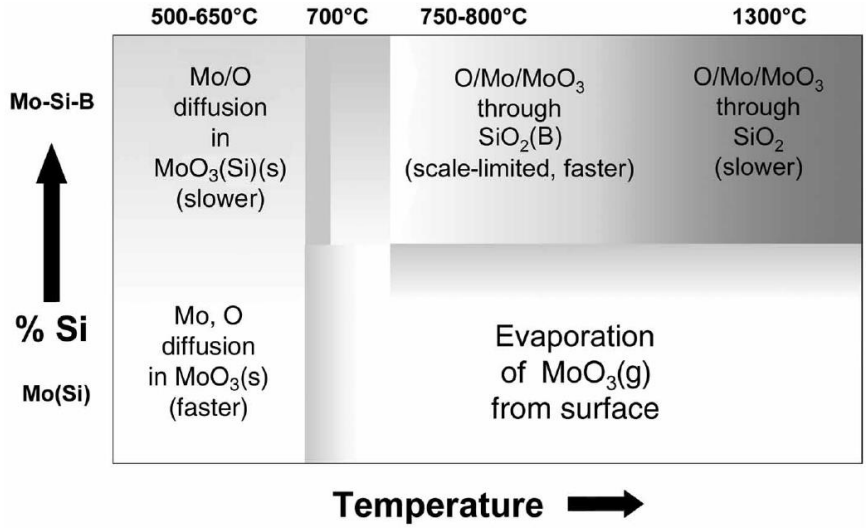

Figure 2.1.3: Oxidation mechanism map in temperature [36].

2.2 Mechanical properties of Mo-Si-B materials

Since boron addition has been known to increase the oxidation resistance of Mo-Si materials it is important to determine the mechanical properties of the resulting products.

Akinc et al. were able to achieve 97% theoretical density in a Mo-13Si-1.3B at% mixture. This relatively small boron addition led to a compressive creep rate of 140-180 MPa at temperatures between 1220 °C and 1320 °C [11].

In addition, Alur et al. determined the compressive strength at room temperature as well as the yield strength of the alloy with composition Mo-6.1Si-7.9B at%. These characteristics were 1280 MPa and 300 MPa, respectively. Also, they tested the composition Mo-8.6Si-8.7B and obtained the multi-phase material Mo-MoB-Mo_5Si_3-Mo_5SiB_2 and stated that the fracture toughness increased as the concentration of Mo increased [37].

Subsequently, Li et al. were able to synthesize a Mo-MoB-Mo_5Si_3-Mo_5SiB_2 by utilizing the Mo-12Si-8.5B wt% composition (Figure 2.2.1). The compressive strength was 2445 MPa. Meanwhile, the yield stress and fracture toughness at room temperature were 1915 MPa and 8.77 MPa $m^{1/2}$, respectively [38].

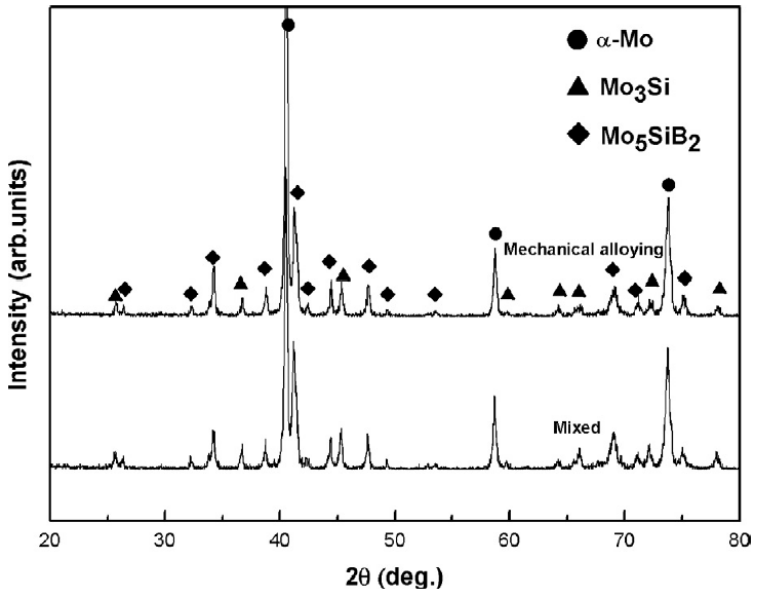

Figure 2.2.1: XRD patterns after mixing and after mechanical alloying [38].

Biragoni et al. were able to calculate the elastic and shear modulus, Poisson's ratio, and the bulk modulus of Mo-12Si-8.5B mixtures at different temperatures. They found that at room temperature, these materials possess an elastic modulus of 325 GPa, a shear modulus of 126 GPa, a Poisson's ratio of 0.285, and a bulk modulus of 252 GPa. At 1200 °C these characteristics were 269 GPa, 102 GPa, 0.312, and 239 GPa, respectively [39]. Based on these data, Mo-12Si-8.5B composition is considered as a promising Mo-Si-B alloy.

Choe et al. have analyzed these materials with scanning electron microscopy and shown that Mo_3Si and Mo_5SiB_2 phases are embedded in a continuous α-Mo matrix (Figure 2.2.2). This matrix toughens the material that originally lost ductility because of the addition of compositions that promote oxidation resistance (i.e. B and Si) [13].

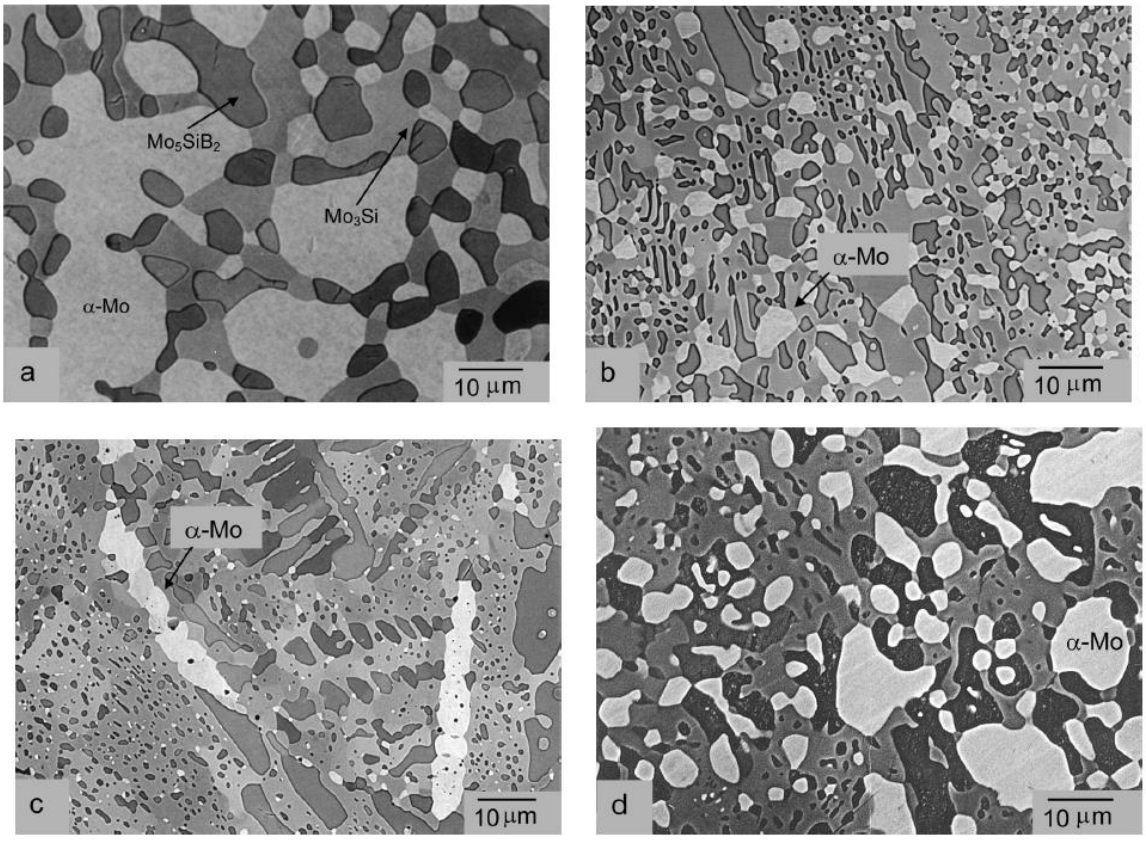

Figure 2.2.2: Scanning electron micrographs of the microstructures in the Mo-Si-B alloys [13].

In another work, Choe et al. demonstrated that this matrix increased the fracture toughness at elevated temperatures delivering values of over 10 MPa $m^{1/2}$ at 1200 °C and 11.8 MPa-$m^{1/2}$ at 1300 °C. Also, they stated that the α-Mo matrix is the main phase in the toughening of the alloy trapping and stopping the crack motion (Figure 2.2.3) [30].

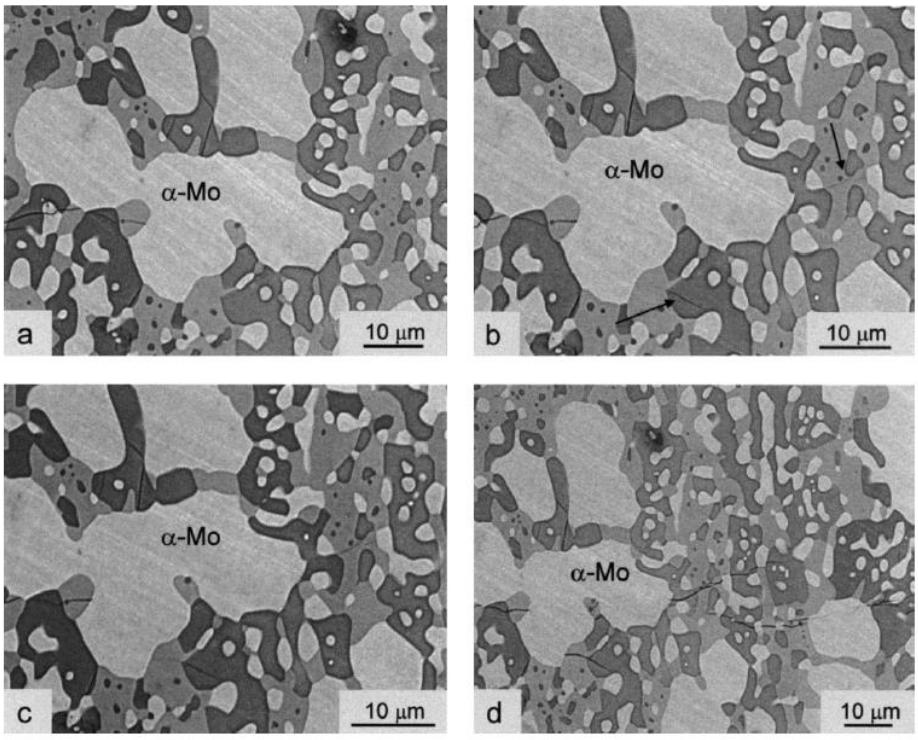

Figure 2.2.3: In situ scanning electron micrographs illustrating the development of microcracking ahead of the crack tip during the extension of the main crack [30].

Kruger et al. have also investigated the effects of Mo matrix. Compositions of Mo-8B, Mo-25Si, Mo-4Si-2B, Mo-6Si-5B, Mo-13Si-12B, Mo-9Si-8B were tested. It was found that the Mo matrix decreases the ductile-to-brittle transition by 150 K [14]. In another work, Kruger et al. found that higher concentrations of Mo deliver the highest fracture toughness. For compositions of Mo-6Si-5B, the obtained fracture toughness was as high as 13.6 MPa·$m^{1/2}$ [29].

Kruzic et al. have investigated the crack path in the three-phase alloys. They found that the crack path was impeded by the continuous molybdenum matrix. Figure 2.2.4 shows the crack path [40].

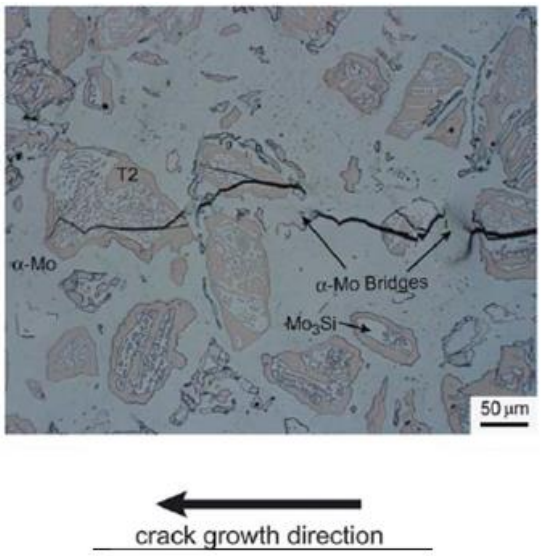

Figure 2.2.4: Crack trapping and bridging at the α-Mo phase in the "coarse" Mo-Si-B alloy [41].

2.3 Mo_5SiB_2 phase

Mo_5SiB_2, also known as T_2 phase, is formed by a unit cell of 32 atoms (20 Mo, 4 Si, 8 B). The crystal structure is body-centered tetragonal. Figure 2.3.1 depicts the crystal structure of T_2.

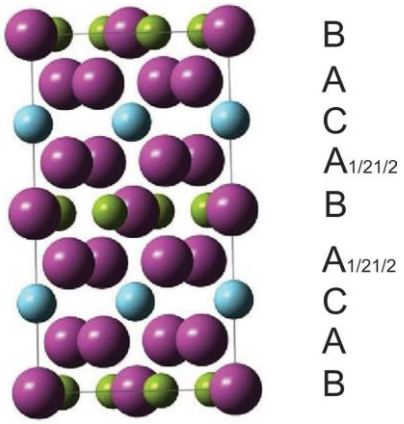

Figure 2.3.1: Crystal structure of Mo_5SiB_2 [9].

The atoms are arranged in the BACA BA CAB configuration where layer A only contains Mo atoms, layer B contains Si atoms, and layer C contains Mo and B atoms [9].

Mo_5SiB_2 has higher mechanical properties than other molybdenum silicides. It possesses an elastic modulus of 383 GPa, a shear modulus of 151 GPa, hardness of 18 GPa, and a fracture toughness as high as 2.0 MPa $m^{1/2}$ [42].

Ito et al. tested T_2 single crystals at elevated temperatures. They found that these crystals were plastically deformable at 1500 °C with a stress of 432 MPa. This means that at such high temperatures the creep rate was stress dependent [43].

2.4 Mo_5SiB_2-TiC material

One way to toughen these molybdenum borosilicides is by adding secondary phases such as TiC. This additive is attractive because of its high melting point of 3160 °C and a relatively low density of 4.93 g/cm^3 [16]. The addition of TiC is a relatively new method and little research has been made. However, Shimpei et al. found that adding 7.5 at% of TiC to the main Mo-Si-B network (70Mo-5Si-10B-7.5B) greatly improves the compressive strength of the molybdenum borosilicides at temperature of 1600 °C [17].

Chapter 3: Experimental Procedures and Facilities

3.1 Sample preparation

Molybdenum (99.95% pure, Climax Molybdenum), silicon (crystalline, 99.95% pure, Alfa Aesar), boron (amorphous, 94-96% pure, Alfa Aesar), graphite (crystalline, 99% pure, Alfa Aesar), and titanium (99.5% pure, Alfa Aesar) powders were used in the present study.

The powders were mixed in a three-dimensional inversion kinematics mixer (Inversina 2L, Bioengineering, Inc) (Figure 3.1.1) for 1 hour at 70% of the maximum speed. The usual amount of powder mixed was about 50 g.

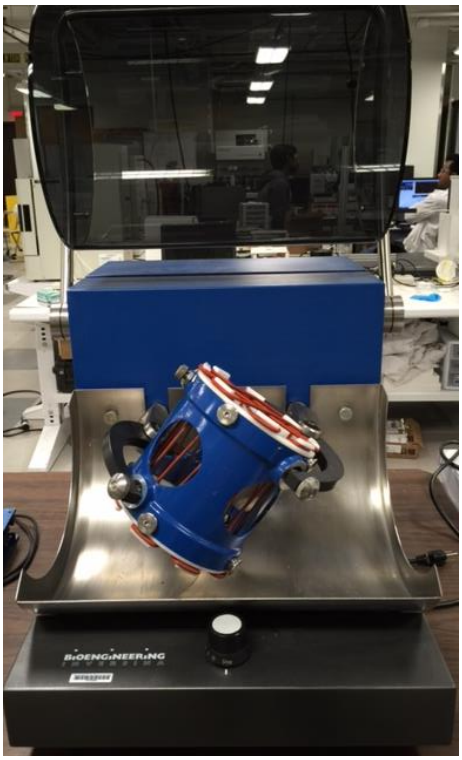

Figure 3.1.1: Three-dimensional inversion kinematics mixer (Inversina 2L).

Then, the mixture was milled in a planetary ball mill (Fritsch Pulverisette 7 Premium line) using 80 mL zirconia coated bowls (Figure 3.1.2). The grinding media consisted of 1.5-mm zirconia balls and the ball-mixture weight ratio was 6:1. The milling process was conducted at the maximum speed of 1100 rpm in an ultra-high purity argon environment to avoid oxidation by

atmospheric air. The milling time was 10 min and it was followed by a 75-min cooling process to avoid overheating of both the bowls and the mixture. The procedure included 4 milling-cooling cycles.

Figure 3.1.2: Fritsch Pulverisette 7 Premium line (left) and 80 mL zirconia coated bowls (right).

The as-milled powders were analyzed using X-ray diffraction (Bruker D8 Discover XRD) to ensure the powders did not react during the milling process. Then, the powders were compacted into cylindrical pellets using a uniaxial hydraulic press (Carver) and a 13-mm pellet die (Figure 3.1.3). To fabricate materials by conventional SHS, the pressing force was 40 kN. The height of pellet varied, ranging from 10 mm to 22 mm. A 3-mm-tall booster mixture of stoichiometric Ti-B (1:2 mole ratio) was placed on the top of the pellet to aid the ignition. The relative densities of the main pellets ranged from 57-66%.

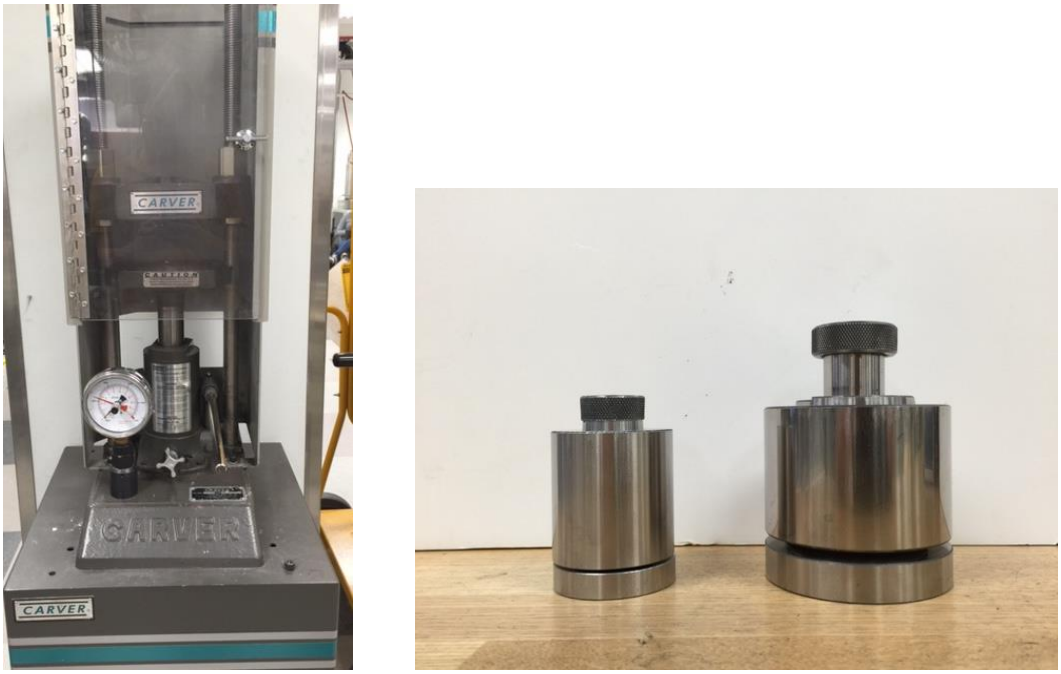

Figure 3.1.3: Uniaxial hydraulic press (Carver), 13-mm die, and 25-mm die.

In the chemical oven technique, a composite pellet with the main mixture as core and the booster mixture as shell was fabricated (Figure 3.1.4). The main pellet was compacted in a 13 mm die, submerged into a Ti-B mixture (1:2 mol ratio) inside a 25-mm die, and pressed again using a lesser force of 20-25 kN. The height of the resulting composite pellet was 23-26 mm. To avoid heat losses during combustion, the pellet was wrapped by 3-mm-thick thermal paper (Fiberfrax).

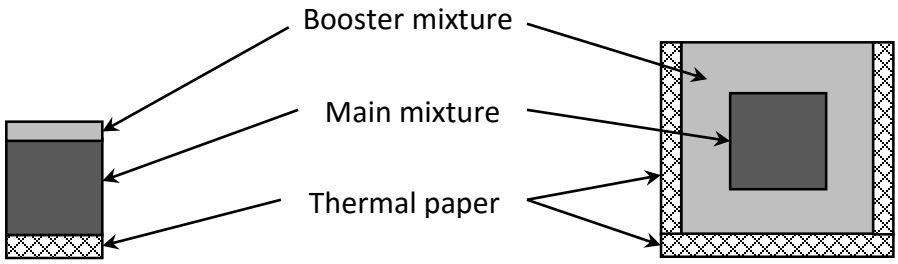

Figure 3.1.4: Sketches of pellets prepared for conventional SHS (left) and chemical oven experiments (right) [44].

3.1.1 Preparation of α-Mo-Mo_3Si-Mo_5SiB_2 materials

To fabricate materials containing α-Mo-Mo_3Si-Mo_5SiB_2 phases, a mixture of Mo (79.5 at%), Si (12.0 at%), and B (8.5 at%) was prepared. The mixture is designed to obtain only the desired three phases.

3.1.2 Preparation of Mo_5SiB_2-TiB_2 materials

To fabricate materials based on Mo_5SiB_2-TiB_2 phases, five compositions were tested. The resulting mixture consisted of 10 wt%, 15 wt%, 20 wt%, 30 wt%, and 40 wt% of stoichiometric Ti-B (1:2 mol ratio) and stoichiometric Mo-Si-B (5:1:2 mol ratio) as the main mixture.

For the chemical oven experiments, the composition was the mixture designed for 15 wt% TiB_2.

3.1.3 Preparation of Mo_5SiB_2-TiC materials.

To fabricate materials based on Mo_5SiB_2-TiC phases, four compositions were tested. The resulting mixture consisted of 10 wt%, 20 wt%, 30 wt%, and 40 wt% of stoichiometric Ti-C (1:1 mol ratio) and stoichiometric Mo-Si-B (5:1:2 mol ratio) as the main mixture.

For the chemical oven experiments, the composition was the mixture designed for 15 wt%-TiC.

3.2 Combustion experiments

All combustion experiments were performed in a 30-L stainless steel reaction chamber. The pellet was placed vertically on a ceramic fiber insulation (Fiberfrax). The chamber was evacuated three times using a vacuum pump (Fisher Scientific, Maxima C Plus) and filled with ultrahigh purity argon at 1 atm. Since the pressure in the lab is usually around 890 mbar, the

pressure inside the chamber was set at the 2-psi mark in the pressure gage (138 mbar), so that the absolute pressure in the chamber was approximately equal to 1 atm.

The mixture was ignited by a 0.43-mm-diameter tungsten wire coil (Midwest Tungsten Service Inc.), connected to a DC power supply (Mastech) using 12 W of power. After ignition, the power supply was shut off. WRe5%/WRe26% thermocouples (type C, wire diameter: 76 µm, Omega Engineering), located in two-channel ceramic insulators, were inserted into pellets through drilled channels. The thermocouples were connected to a USB-based data acquisition system (National Instruments USB-9211).

A high-speed video camera (Vision Research Phantom v1210), equipped with a lens for macro shooting (Nikon AF Micro NIKKOR 60 mm f/2.8D), was used for observations of the combustion process through a glass window. The resolution used was 1024 × 768 with a frame rate of 500 fps. The experimental setup is shown in Figure 3.2.1

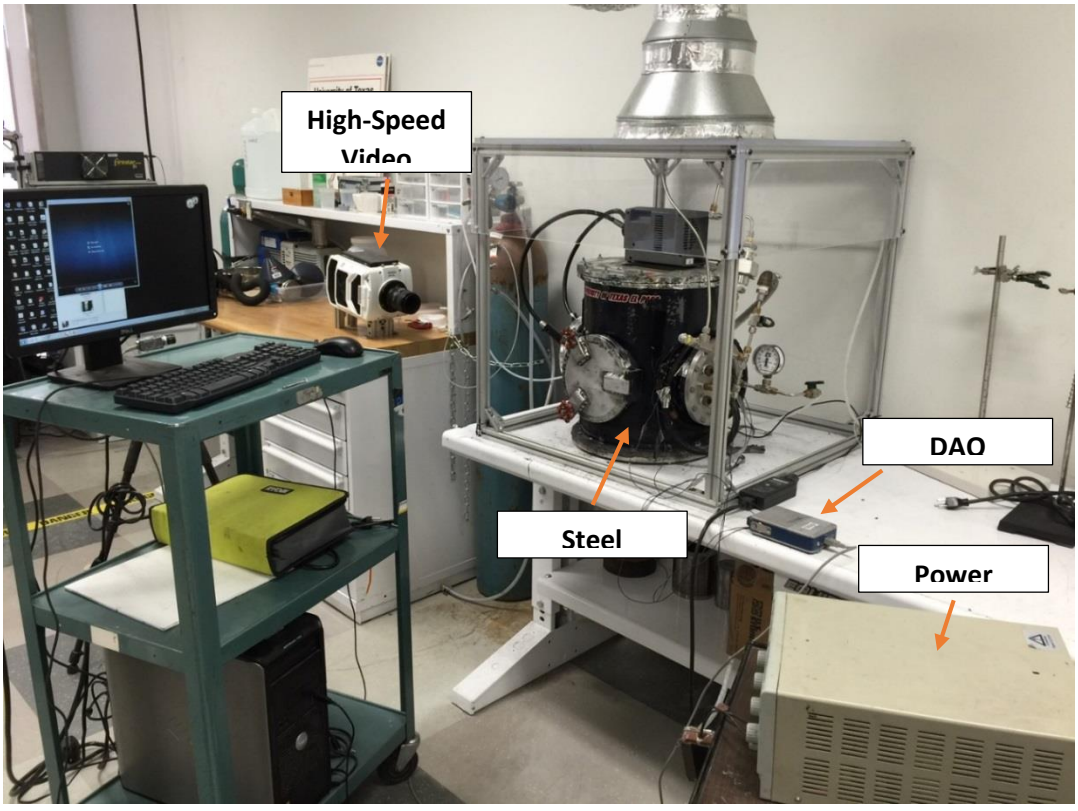

Figure 3.2.1: Experimental setup for SHS and chemical oven experiments.

3.2.1 Mechanically activated self-propagating high temperature synthesis (MASHS)

During MASHS combustion experiments, fast combustion of the booster pellet was observed, which led to a self-sustained propagation of the combustion front over the entire pellet. The power supply was shut off after ignition of the booster mixture, so no external energy was added to complete the combustion.

The booster mixture, Ti-B (1:2 mol ratio), has an enthalpy of formation of −279.49 kJ/mol [45] and an adiabatic flame temperature of 3193 K [46]. These properties are sufficient to sustain the combustion of the main Mo-Si-B mixture.

In some cases, the released heat by the main mixture was not sufficient for maintaining a planar combustion front and the spin combustion regime was observed instead. This phenomenon occurs in some low-exothermic mixtures where multiple hot spots can be observed along the surface of the pellet [47], [48], [49], and [50].

3.2.2 Chemical oven combustion technique

During chemical oven combustion, fast and violent combustion of the booster shell was observed. The total quantity of booster mixture, the adiabatic flame temperature, and the use of insulator around the composite pellet delivered enough heat to allow even the lowest exothermic mixtures in the present study to burn.

After combustion and cooling, the shell is easily removed and does not react with the main mixture. Usually, the products presented visible cracks on the top of the pellet, presumably associated with processes during pressing of the composite pellet.

3.3 Characterization of products

3.3.1 X-ray diffraction analysis

Tthe X-ray diffraction analysis was used to examine the as-milled powders in search for unwanted reactions during milling and to characterize the phases in the combustion products. Figure 3.3.1.1 shows the used instrument (Bruker D8 Discover XRD with Cu K-alpha radiation). The products were crushed into powder and then analyzed at different 2θ values, ranging from 20° to 90°.

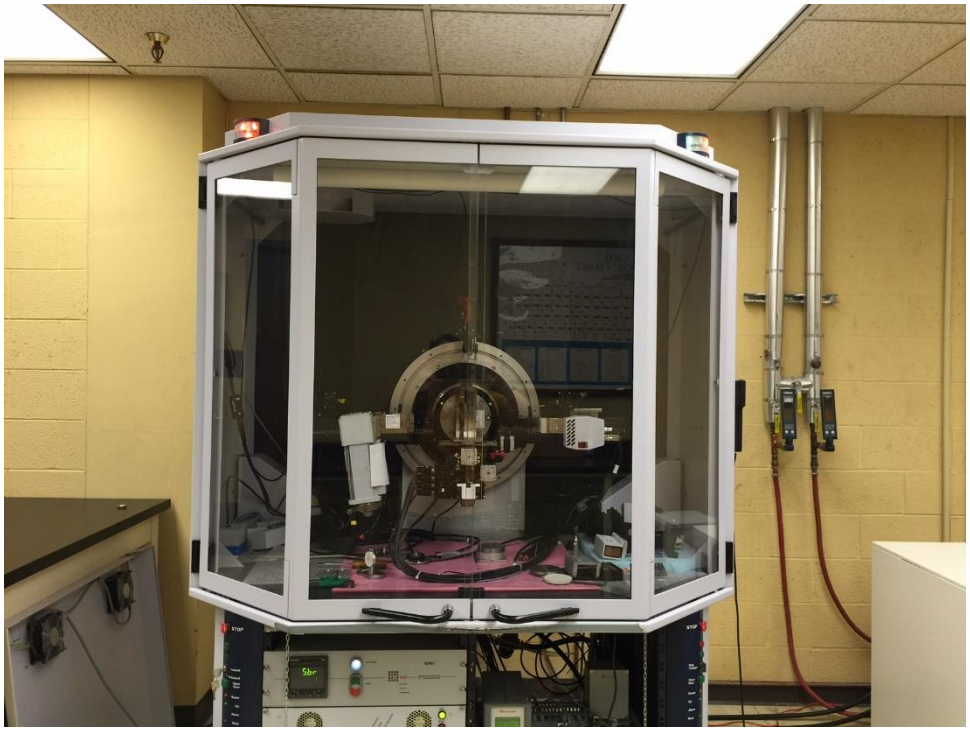

Figure 3.3.1.1: Bruker D8 Discover XRD.

3.3.2 Thermogravimetric analysis (TGA)

One of the goals of this project is to investigate the oxidation resistance of the obtained products. The Netzsh TGA 209 F1 Iris thermogravimetric analyzer (Figure 3.3.2.1) was used to study the oxidation resistance of the obtained products at temperatures up to 1000 °C. TGA consists in analyzing the transient mass change of the sample at different temperatures.

Alumina crucibles (inner diameter 5.85-mm) were used to hold the samples with masses from 10 mg to 69 mg. The oxidation experiments were performed in an oxygen-argon environment consisting of 20% O_2 and 80% Ar with flow rates of 6 mL/min and 24 mL/min, respectively. The heating rate was 10 °C/min.

Figure 3.3.2.1: Netzsh TGA 209 F1 Iris thermogravimetric analyzer.

3.3.3 Differential scanning calorimeter (DSC)

Due to the temperature limitations of the TGA, the Netzsch DSC 404 F1 Pegasus differential scanning calorimeter (Figure 3.3.3.1) was used to study the oxidation resistance of the products at temperatures up to 1500 °C. Unlike TGA, DSC does not provide information on the mass change of the sample, but it gives information on the released or consumed heat. In this study, exothermic reactions, such as oxidation, are depicted as positive peaks, while endothermic reactions are shown as negative peaks.

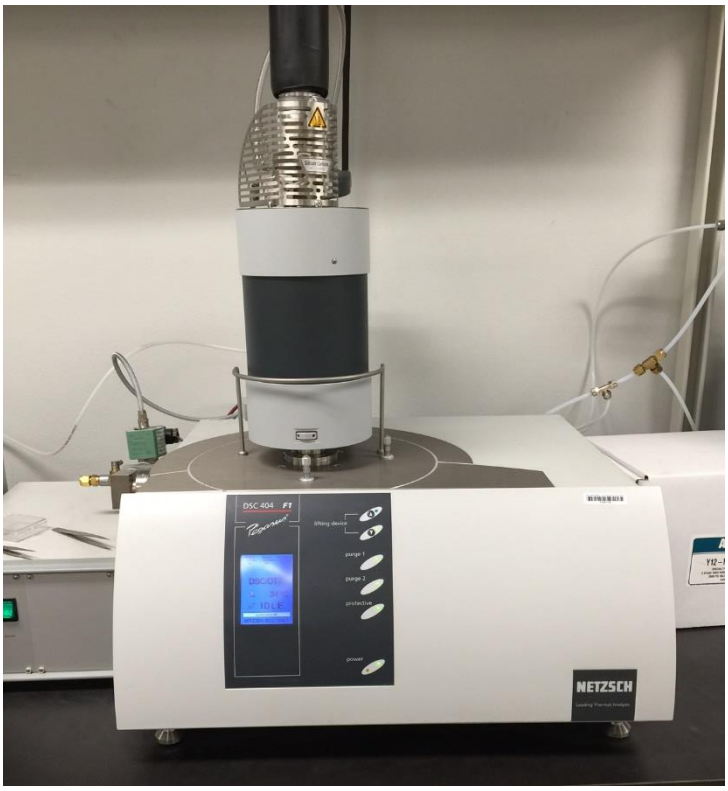

Figure 3.3.3.1: Netzsh DSC 404 F1 Pegasus differential scanning calorimeter.

As in the TGA tests, 5.85-mm alumina crucible were used to hold the samples with masses from 10 to 69 mg. The oxidation experiments were performed in an oxygen-argon environment consisting of 20% O_2 and 80% Ar with flow rates of 6 mL/min and 24 mL/min, respectively. The heating rate used 10 °C/min.

3.3.4 Compression test

To determine the compressive strength, the INSTRON 5866 testing machine was used (Figure 3.3.4.1). The displacement rate was 5 mm/min. The compressive strength of the product was calculated from stress-strain curve obtained in the test.

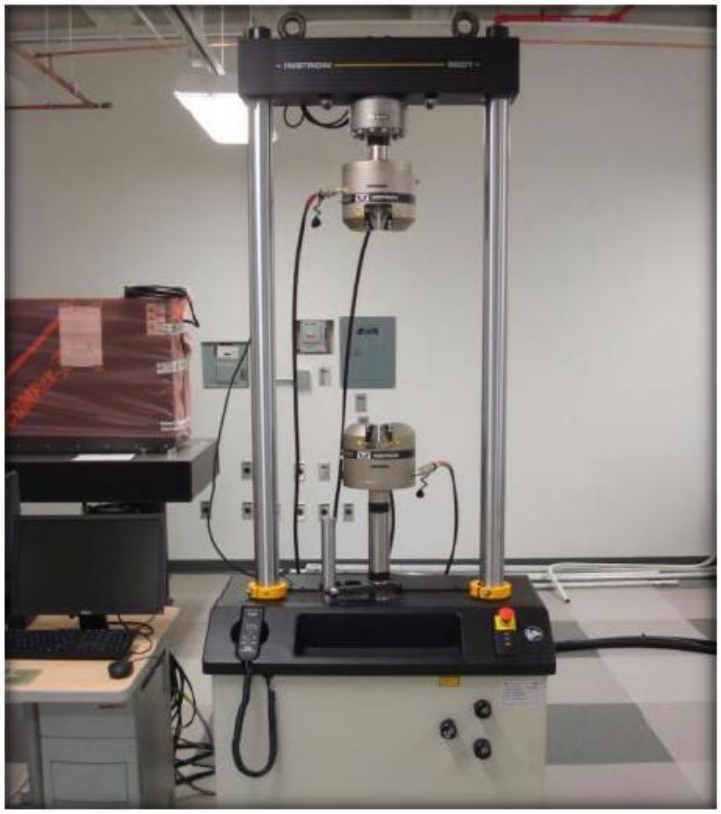

Figure 3.3.4.1: INSTRON 5866 testing machine.

3.3.5 Nano indentation tests

To determine the elastic modulus and hardness of the material, the Hysitron TI 750H Ubi nanomechanical test instrument was used (Figure 3.3.5.1). The nanoindentator made around 36 impacts on each sample at room temperature. The properties presented in this study are the average results of every impact. This nanoindentator is capable of calculating the hardness of the material directly. Also, the elastic modulus is determined by the following equation,

$$E = \frac{1}{E_r} - \frac{1140}{1 - 0.07^2}$$

Figure 3.3.5.1: Hysitron TI 750H Ubi nanomechanical test instrument.

Chapter 4: Results and Discussion

4.1 Mo_5SiB_2-TiC materials fabricated by MASHS

As it was previously stated, four compositions (10 wt%, 20 wt%, 30 wt%, and 40 wt%) of stoichiometric Ti/C (1:1 mol ratio) were added to the main mixture of stoichiometric Mo_5SiB_2 (5:1:2 mol ratio). Efforts were made to ignite the mixture using a booster mixture (Ti/B, 1:2 mol ratio) on the top of the pellet. The booster mixture ignited, but the main mixture did not.

4.2 Mo_5SiB_2-TiB_2 materials fabricated by MASHS

Five compositions (10 wt%, 15 wt%, 20 wt%, 30 wt%, and 40 wt%) of stoichiometric Ti/B (1:2 mol ratio) were added to the main mixture of stoichiometric Mo_5SiB_2 (5:1:2 mol ratio). A booster mixture was placed on the top of each pellet. Almost all experiments were successful. The combustion behavior was different depending on the composition.

The first composition tested was Mo_5SiB_2-10% TiB_2. The mixture ignited, but the combustion front stopped in the middle of the pellet. In Figure 4.2.1 it is seen that when the combustion front reaches the middle of the pellet, two hot spots moving in opposite directions along the front appear on the pellet surface. Therefore, the combustion front is planar at the beginning of the propagation, but heat losses lead to spin combustion.

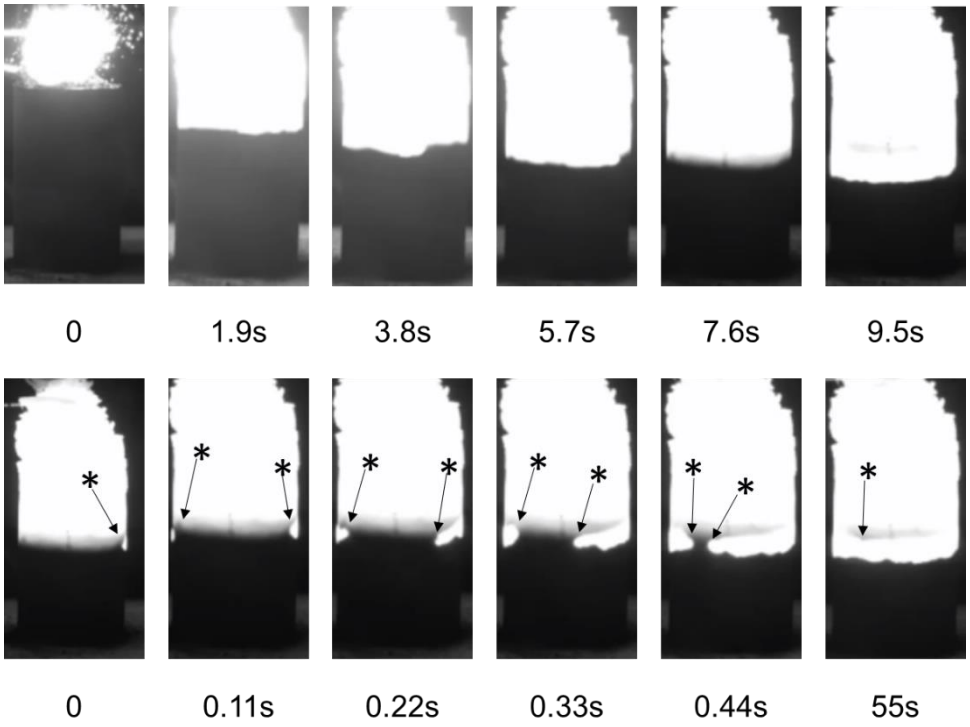

Figure 4.2.1: Combustion of Mo-Si-B-Ti mixture designed for 90% Mo_5SiB_2 and 10% TiB_2.

The second composition tested was the mixture designed for 15 wt% TiB_2. Figure 4.2.2 shows the combustion propagation over this mixture. It is seen from the top series of images that the combustion front propagates downward with an approximately constant axial velocity (about 4 mm/s). The bottom series of images in Fig. 1 reveals a spinning structure of the combustion wave. Specifically, a counter-propagating motion is seen in the images with time labels 0.08 s and 0.1 s.

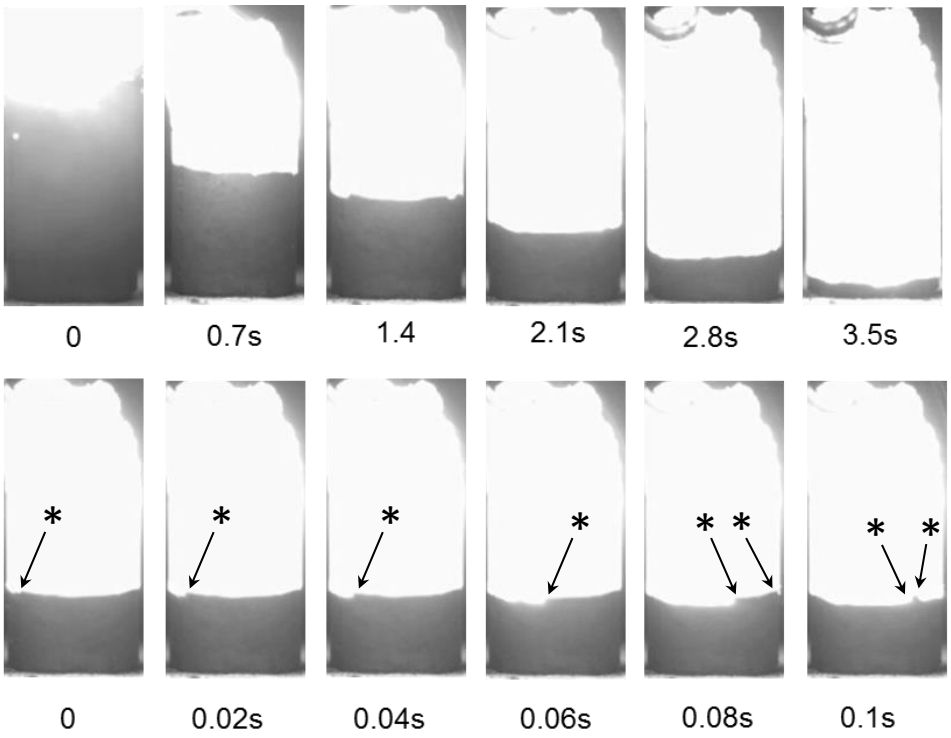

Figure 4.2.2: Combustion of Mo-Si-B-Ti mixture designed for 85% Mo_5SiB_2 and 15% TiB_2 [44].

The mixture designed for 20 wt% TiB_2 was the third composition tested. The combustion was different from the previous two. Upon ignition of the booster pellet, the main mixture exhibited a fast and uniform planar combustion. The main pellet completely burned, but the reaction was so violent that the pellet was split into two parts near the base (Figure 4.2.3).

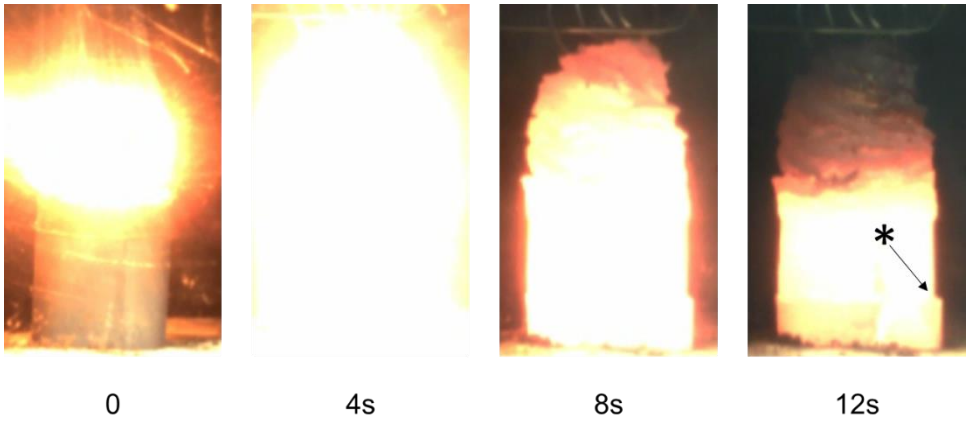

Figure 4.2.3: Combustion of Mo-Si-B-Ti mixture designed for 80% Mo_5SiB_2 and 20% TiB_2.

The fourth combustion experiment was with the mixture designed for 30 wt% TiB_2. The combustion is similar to the mixture designed for 20 wt%: fast and uniform propagation of the planar combustion front. However, the combustion product exhibited cracks along its height, apparently due to the high energy of the combustion (Figure 4.2.4).

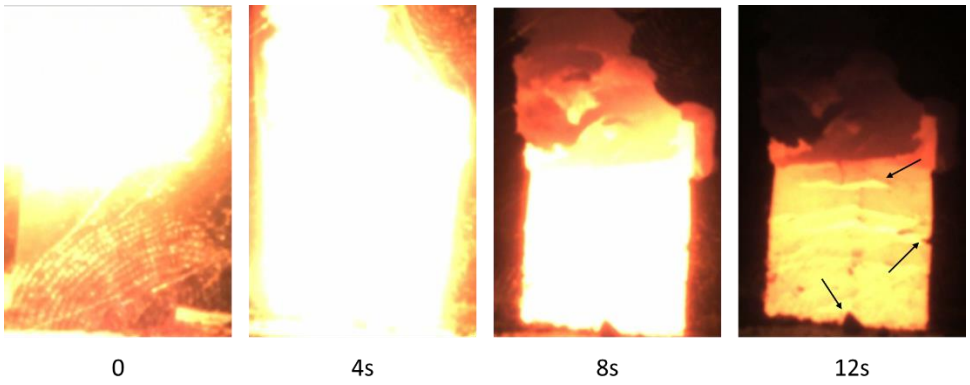

Figure 4.2.4: Combustion of Mo-Si-B-Ti mixture designed for 70% Mo_5SiB_2 and 30% TiB_2.

The last composition tested was the mixture designed for 40 wt% TiB_2. The combustion front was planar, but it was constantly interrupted by the pellet splitting along the process (Figure 4.2.5).

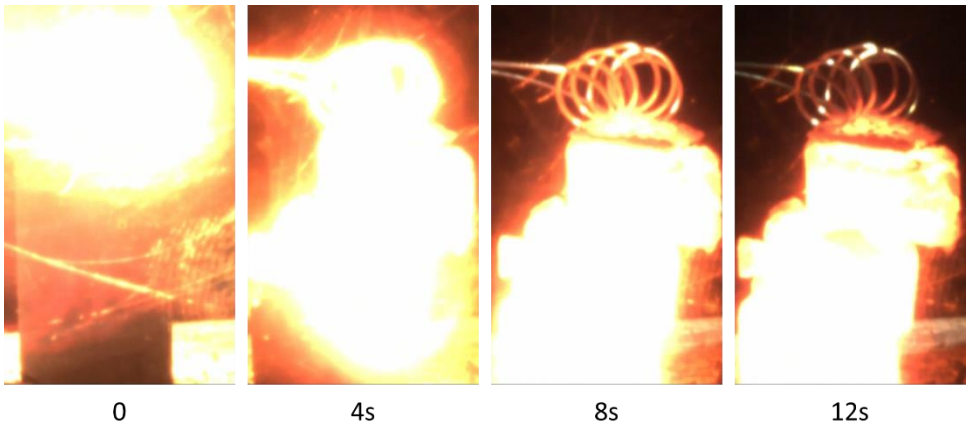

Figure 4.2.5: Combustion of Mo-Si-B-Ti mixture designed for 60% Mo_5SiB_2 and 40% TiB_2.

It is seen that as the content of the secondary mixture increased, the combustion was faster and more violent. This excess of energy brought as a consequence cracked combustion products. However, high exothermicities and high combustion temperatures are needed in order to decrease the formation of unwanted phases.

On the other hand, one of the goals of this project is to explore the feasibility of using MASHS for fabricating Mo_5SiB_2-TiB_2 materials. It has been shown that materials with compositions higher than 15 wt% TiB_2 were damaged during MASHS. This means that MASHS is not a viable technique to fabricate materials with high concentrations of this secondary mixture. For this reason, further investigation was made to materials with composition of 15 wt% TiB_2.

The temperature readings in Figure 4.2.6 shows that the maximum temperature achieved during MASHS for the mixture designed for 15 wt% TiB_2 was about 1140 °C. The temperature fluctuates around this temperature for about 4 s and then it starts to cool for 50 s. The maximum temperature is lower than the melting point of any of the reactants. This means that the reaction mechanism is solid-solid combustion leading to a relatively slow flame propagation [45].

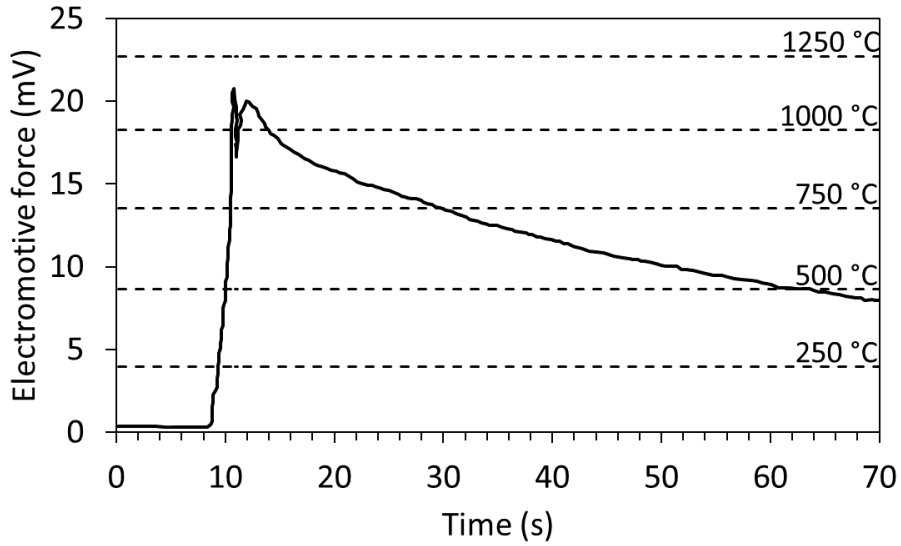

Figure 4.2.6: Time variation of the electromotive force (relative to 0 °C) generated by a C-type thermocouple during combustion (SHS) of Mo/Si/B/Ti mixture designed for 85% Mo_5SiB_2 and 15% TiB_2.

The combustion products had relatively low densities. Figure 4.2.7 shows the combustion product after conventional SHS. Visible pores and cracks can be seen on the surface of the pellet (the top layer consisted of the remains of the booster mixture). The density of the product obtained by conventional SHS was 4.0 g/cm^3.

Figure 2.4.7: Combustion products of Mo/Si/B/Ti mixture designed for 85% Mo5SiB2 and 15% TiB_2 by conventional SHS

These visible defects and the low density determined that SHS may not be adequate to fabricate these materials. For reference, the theoretical density of this material is 8.2 g/cm^3. This means that the relative density obtained was about 50%. Thus, the products fabricated with MASHS do not deliver fully dense materials. However, there are other alternatives explored in this project to fabricate the desired materials.

4.2.1 X-ray diffraction analysis of Mo_5SiB_2-TiB_2 materials fabricated by MASHS

Mo_5SiB_2-TiB_2 materials fabricated by MASHS were characterized using X-ray diffraction analysis. As mentioned above, five different amounts (10 wt%, 15 wt%, 20 wt%, 30 wt%, and 40 wt %) of stoichiometric Ti-B (1:2 mol ratio) were added to the main mixture of stoichiometric Mo-Si-B (5:1:2 mol ratio).

Figure 4.2.1.1 shows the spectrum of the mixture designed for Mo_5SiB_2-10 wt% TiB_2. It is seen that the desired Mo_5SiB_2 and TiB_2 phases were obtained. However, those two phases are accompanied by Mo_5Si_3, Mo, and MoB. It is seen that those three phases have the highest peaks in the spectrum.

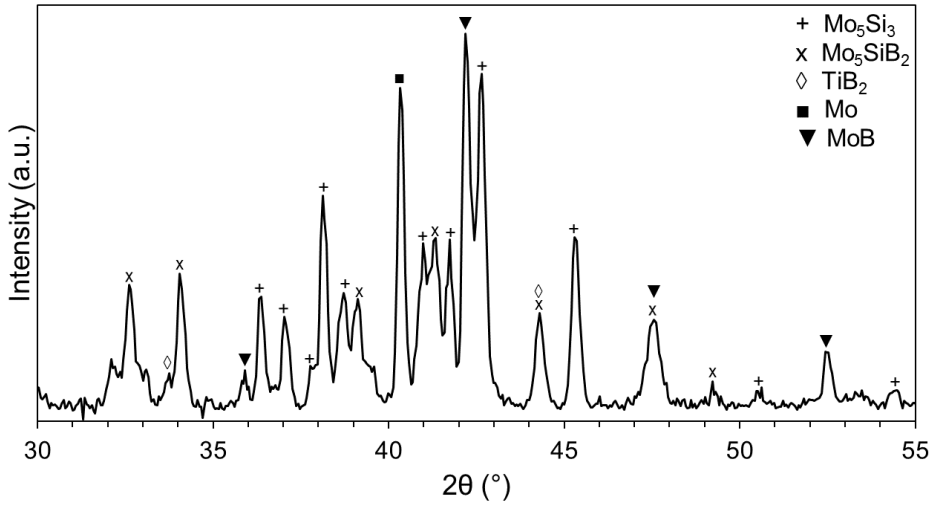

Figure 4.2.1.1: XRD pattern of products obtained by combustion (SHS) of Mo/Si/B/Ti mixture designed for 90% Mo_5SiB_2 and 10% TiB_2.

Figure 4.2.1.2 shows the spectrum for the mixture designed for Mo_5SiB_2-15 wt% TiB_2. Again, the desired Mo_5SiB_2 and TiB_2 were accompanied by Mo, Mo_5Si_3, and MoB phases. However, the highest peak corresponds to T_2 phase, while the height of the Mo peak at 40.6° decreased significantly. Also, the three peaks of Mo_5Si_3 between 41° and 43° completely disappeared. Thus, the two major peaks correspond to T_2 phase and MoB.

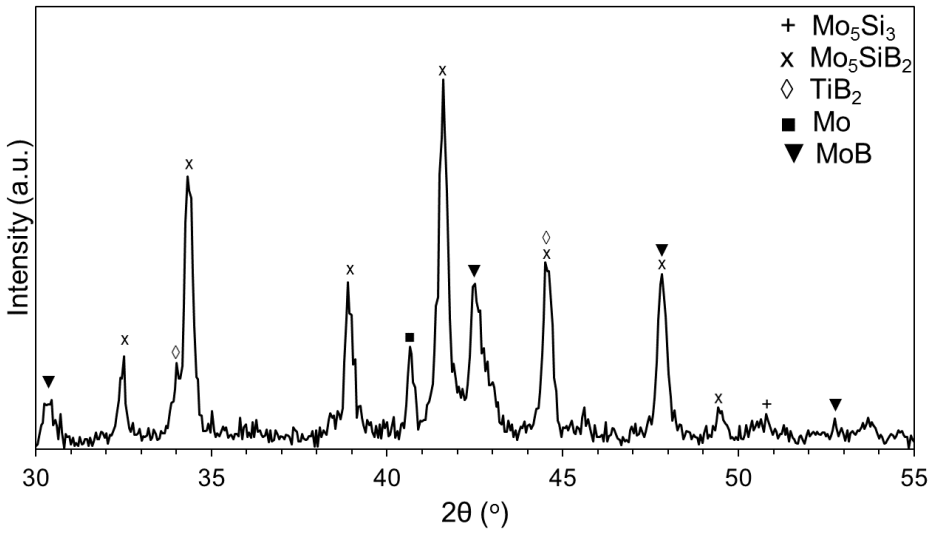

Figure 4.2.1.2: XRD pattern of products obtained by combustion (conventional SHS) of Mo/Si/B/Ti mixture designed for 85% Mo_5SiB_2 and 15% TiB_2.

Figure 4.2.1.3 corresponds to the mixture designed for 20 wt% TiB_2. Again, the desired phases T_2 and TiB_2 were obtained and the highest peak corresponds to the former. However, Mo_5Si_3 phase reappears between 42° and 43° and the MoB was the second highest peak. Also, it can be seen that the Mo peak at 40.6° kept decreasing in height.

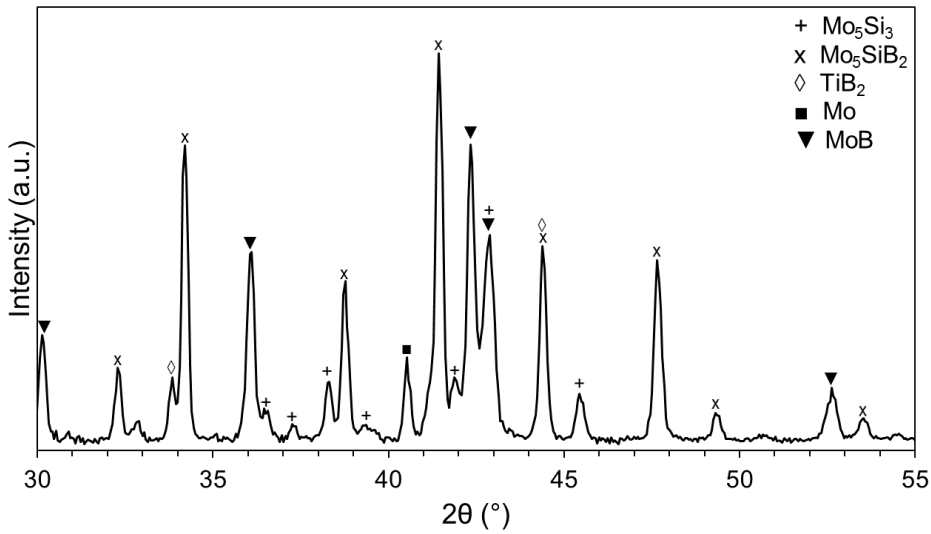

Figure 4.2.1.4: XRD patterns of products obtained by combustion (conventional SHS) of Mo/Si/B/Ti mixture designed for 80% Mo_5SiB_2 and 20% TiB_2 [44].

Likewise, Figure 4.2.1.5 shows the spectrum for the mixture designed for 30 wt% TiB_2. It is observed that the two desired phases, T_2 and TiB_2, were obtained, but the intensity of the Mo peak at 40.6 ° significantly decreased. Also, the main phases were MoB and Mo_5Si_3. This is undesirable due to the fact that the mixture was designed to only contain Mo_5SiB_2 and TiB_2. In fact, T_2 peaks at 32.5° and 53.8° completely disappeared from the spectrum.

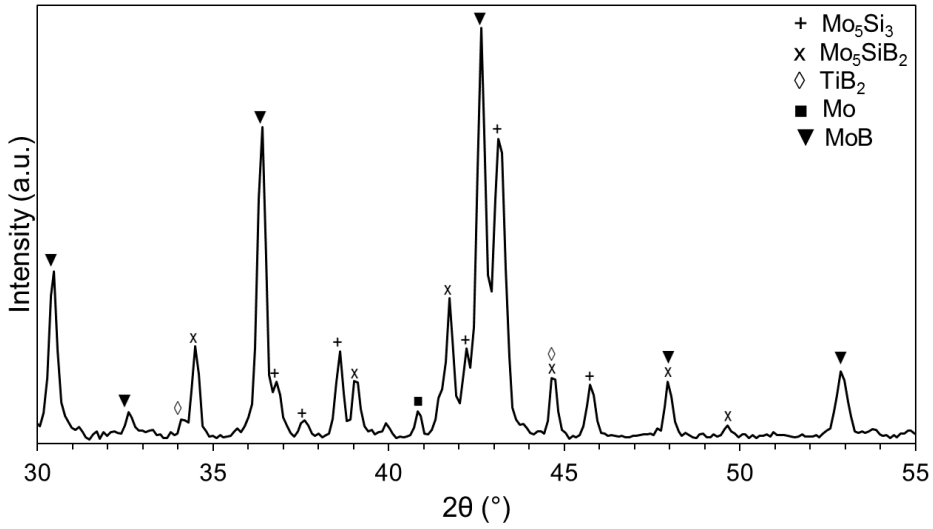

Figure 4.2.1.5: XRD patterns of products obtained by combustion (conventional SHS) of Mo/Si/B/Ti mixture designed for 70% Mo_5SiB_2 and 30% TiB_2.

Lastly, Figure 4.2.1.6 shows the spectrum for the mixture designed for 40 wt% TiB_2. As expected, Mo_5SiB_2 and TiB_2 were obtained. However, the Mo phase completely disappeared and MoB was again the dominant phase. From these spectra, it can be concluded that as the concentration of Ti/B mixture increases, the peak of Mo decreases, which is accompanied by an increase in MoB peaks.

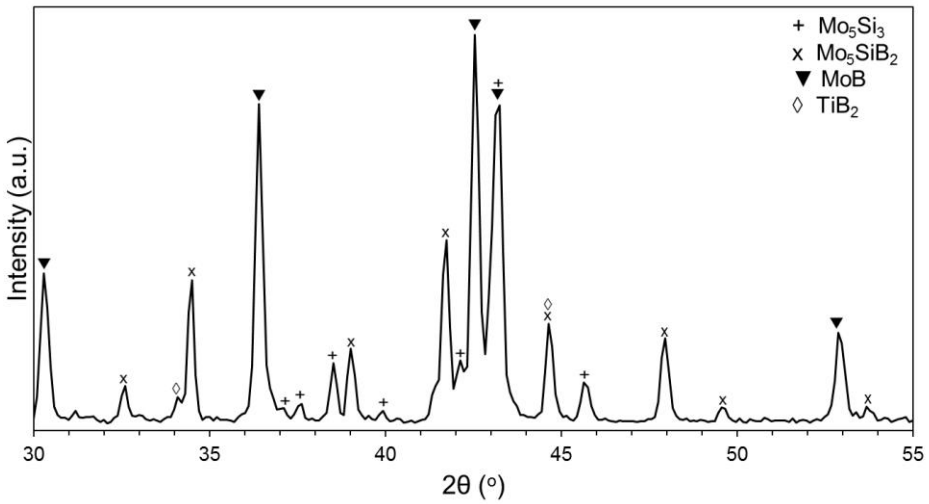

Figure 4.2.1.6: XRD patterns of products obtained by combustion (conventional SHS) of Mo/Si/B/Ti mixture designed for 60% Mo_5SiB_2 and 40% TiB_2.

These results lead to the conclusion that it is impossible to obtain desired two-phase Mo_5SiB_2–TiC and Mo_5SiB_2–TiB_2 materials by a conventional SHS with ignition at the top of the pellet. For this reason, it was decided to focus on the use of the chemical oven technique.

4.2.2 Thermogravimetric analysis of Mo_5SiB_2-TiB_2 materials fabricated by MASHS

Two samples of Mo_5SiB_2-TiB_2 materials with a composition of 15 wt% TiB_2 were tested for oxidation using the thermogravimetric analysis. Figure 4.2.2.1 shows the oxidation behavior of these samples.

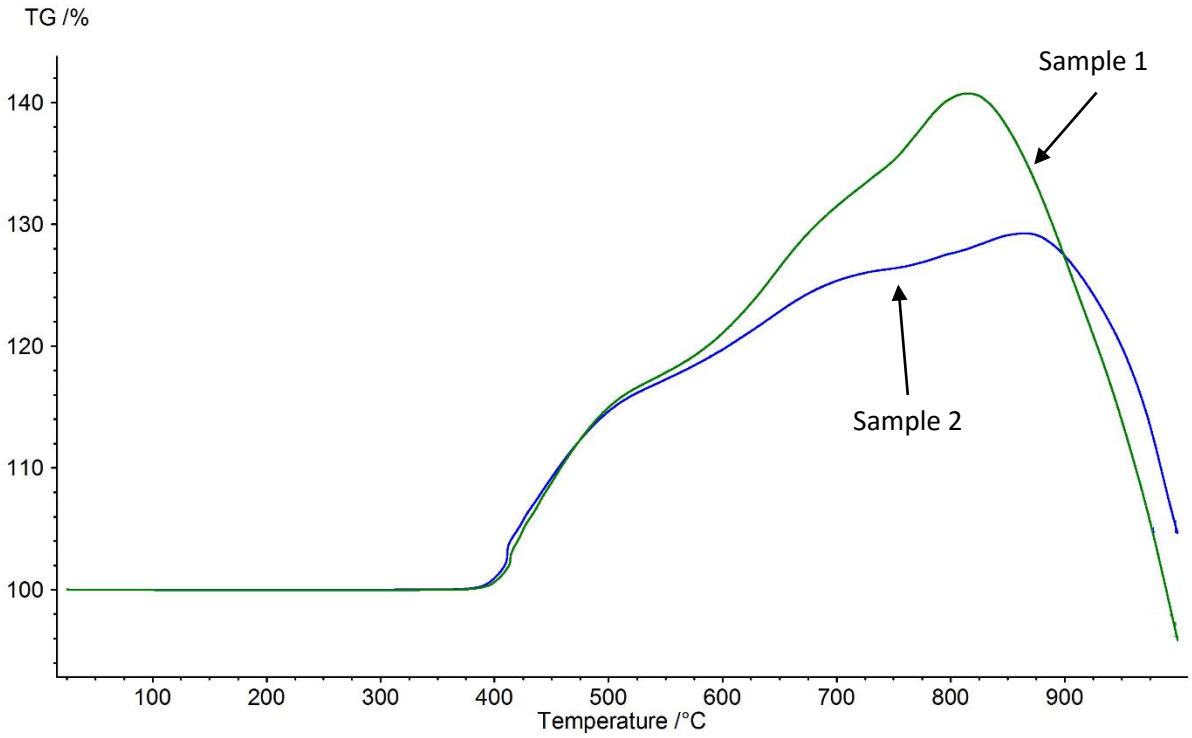

Figure 4.2.2.1: Thermogravimetric curves for samples fabricated by conventional SHS with mixture designed 85% Mo_5SiB_2 and 15% TiB_2.

It is seen that both samples started to gain weight at identical rates at about 400 °C. This trend went on until the 500 °C mark. Sample 1 had a higher oxidation rate and reached its maximum mass gain (40% mass gain) at about 800 °C. However, sample 1 experienced catastrophic mass loss after 800 °C. Likewise, sample 2 experienced a mass gain of about 30% but with a maximum at about 850°C. It exhibited catastrophic mass loss after 850 °C.

4.3 Mo_5SiB_2-TiB_2 materials fabricated by the chemical oven technique

Materials with 15 wt% TiB_2 were fabricated using MASHS. The combustion was stable and the products had minor visible defects. However, the density was relatively low. For this reason, this composition was tested using the chemical oven technique.

The combustion behavior was the same as for the 15 wt% TiC materials. This means that the core pellet burned completely. Figure 4.3.1 shows that the temperature fluctuates around 2400 °C for about 2 s (the combustion stage) and then gradually decreases (the cooling stage). Since the melting points of Mo, Si, B, and Ti are 2623 °C, 1414 °C, 2076 °C, and 1668 °C, respectively, it can be concluded that three of the four reactants (viz. Si, B, and Ti) are liquid in the combustion front, which results in a better conversion to thermodynamically expected products than in the case of conventional SHS where temperatures were below the melting point of Si. During the cooling stage, the temperature drops to 1500 °C for 10 s, to 1000 °C for 25 s, and to 500 °C for 80 s.

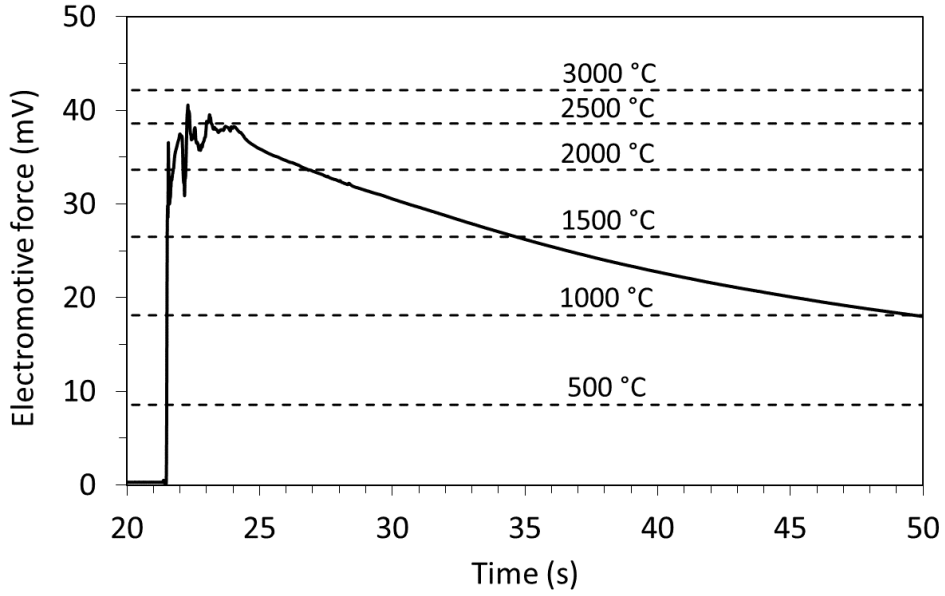

Figure 4.3.1: Time variation of the electromotive force (relative to 0 °C) generated by a C-type thermocouple during combustion (chemical oven) of Mo/Si/B/Ti mixture designed for 85% Mo_5SiB_2 and 15% TiB_2 [44].

Figure 4.3.2 shows that the product has minor visible cracks and has a metallic appearance.

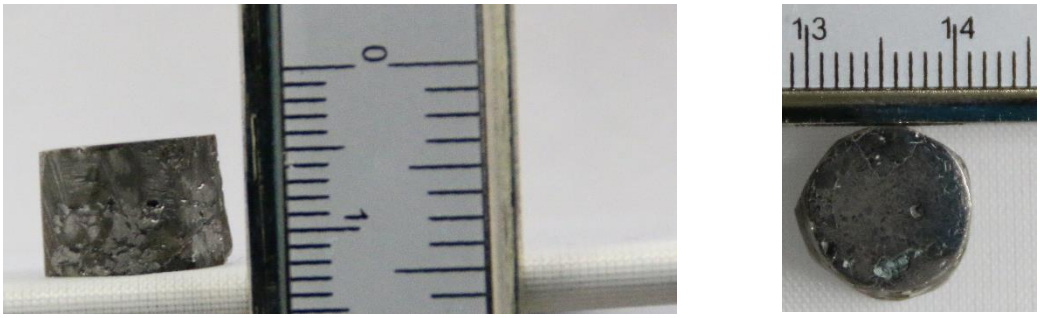

Figure 4.3.2: Combustion products of Mo/Si/B/Ti mixture designed for 85% Mo_5SiB_2 and 15% TiB_2 obtained by the chemical oven technique.

4.3.1 X-ray diffraction analysis of Mo_5SiB_2-TiB_2 materials fabricated using the chemical oven technique

Materials based on Mo_5SiB_2-TiB_2 (a mixture designed for 15 wt% TiB_2) were characterized using X-ray diffraction analysis. Figure 4.3.1.1 shows the typical spectrum for the combustion products for this composition. It is seen that the highest peaks correspond to the desired T_2 and TiB_2 phases. However, these phases are accompanied by a MoB.

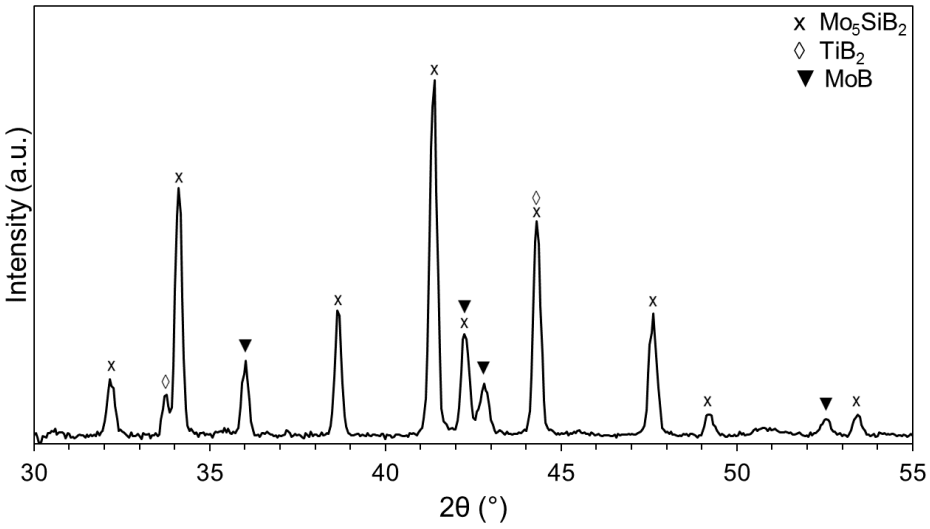

Figure 4.3.1.1: XRD pattern of products obtained by combustion (chemical oven) of Mo/Si/B/Ti mixture designed for 85% Mo_5SiB_2 and 15% TiB_2.

The lower concentrations of secondary phases in these products are likely associated with the higher temperatures during combustion. Thus, the chemical oven technique improved the chemical composition of the products.

The actual density of the product was 6.7 g/cm^3. In other words, the product had a relative density of about 82%. This means that the chemical oven technique improved the density of the MASHS obtained products by 67.5%.

4.3.2 Thermogravimetric analysis of Mo_5SiB_2-TiB_2 materials fabricated using the chemical oven technique

Two samples of Mo_5SiB_2-TiB_2 materials with a composition of 15 wt% TiB_2, obtained with the chemical oven technique, were tested for oxidation using the thermogravimetric analysis. Figure 4.3.2.1 shows the oxidation behavior of these samples.

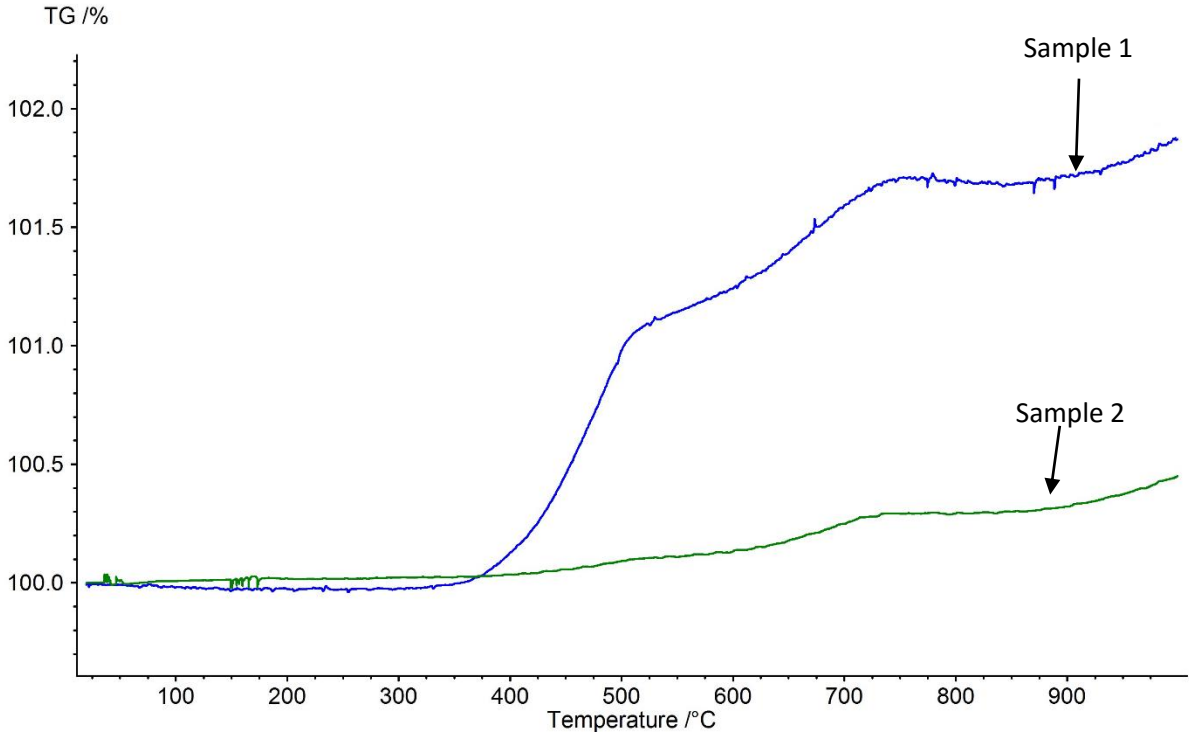

Figure 4.3.2.1: Thermogravimetric curves for samples fabricated by the chemical oven technique with mixture designed 85% Mo_5SiB_2 and 15% TiB_2.

It is seen that sample 1 started to exhibit mass gain at about 380 °C and the mass increased almost linearly until about 500 °C. After that, the oxidation was slower and it stopped at about 750 °C. Then, the mass remained constant until about 900 °C, where the mass started to increase again. Sample 2 experienced a smaller mass change. The oxidation became noticeable at about 400 °C, stopped at about 700 °C, and resumed at about 900 °C.

4.3.3 Differential scanning calorimeter analysis of Mo_5SiB_2-TiB_2 materials fabricated using the chemical oven technique

Two samples of Mo_5SiB_2-TiB_2 materials with a composition of 15 wt% TiB_2, obtained with the chemical oven technique, were tested for oxidation using differential scanning calorimeter. Figure 4.3.3.1 shows the oxidation behavior of these samples at temperatures up to 1500 °C.

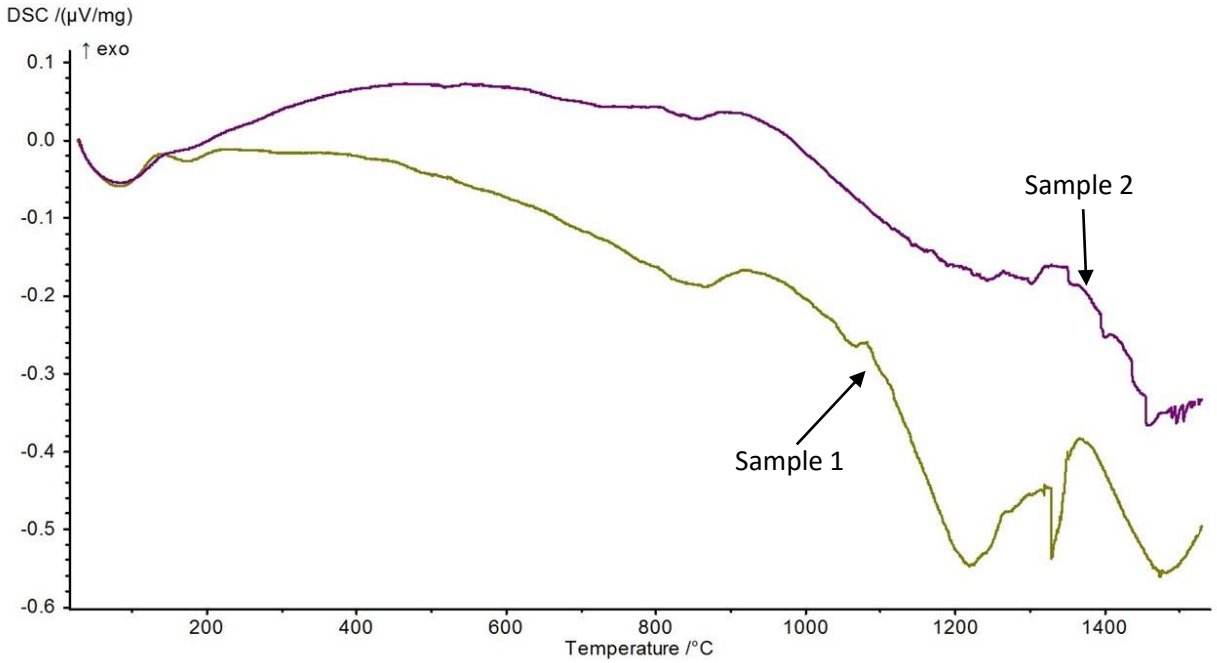

Figure 4.3.3.1: Differential scanning calorimeter curves for samples fabricated by the chemical oven technique with mixture designed 85% Mo_5SiB_2 and 15% TiB_2.

It is seen that sample 1 have very distinct endothermic and exothermic peaks. At 1200 °C, sample exhibited an endothermic peak, apparently due to melting of the material. Then, an exothermic reaction occurred with a maximum at 1300 °C. Generally, the exothermic peaks correspond to oxidation. Immediately, an endothermic reaction took place with its minimum at about 1320 °C. This peak, however, is most likely associated to an error caused by sudden movement of the sample. Then, the second exothermic peak is shown and its maximum is about 1390 °C. Finally, melting occurred after 1400 °C and the correspondent endothermic peak had its maximum at about 1440 °C. On the other hand, sample 2 does not show distinct peaks. However, sample 2 behaved similar to sample 1. In other words, the endothermic and exothermic peaks are similar to those found in sample 1, but the energy of the reaction is less.

4.3.4 X-ray diffraction analysis of the oxidation products of Mo_5SiB_2-TiB_2 materials fabricated using the chemical oven technique

The oxidation products at temperatures of 1000 °C and 1500 °C were analyzed using X-ray diffraction analysis. Figure 4.3.4.1 shows the typical spectrum of the oxidation products at 1000 °C.

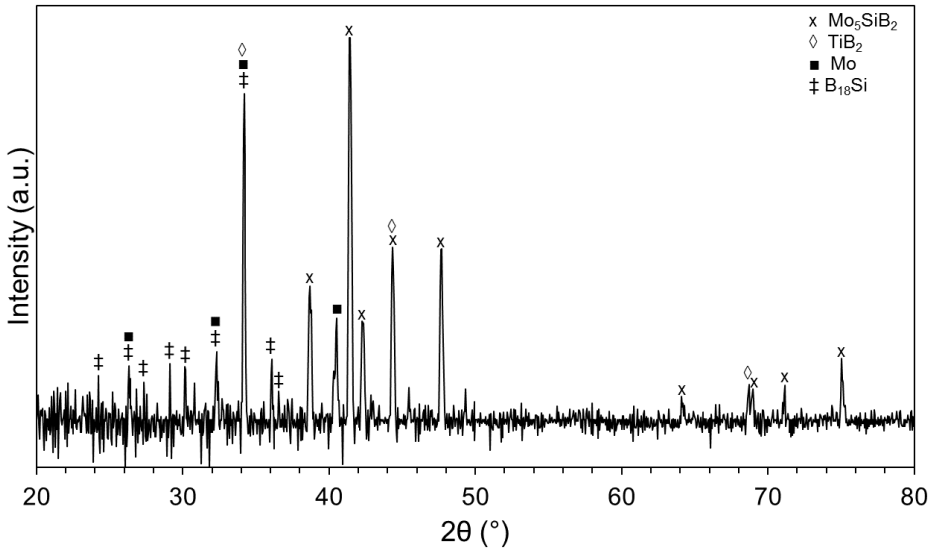

Figure 4.3.4.2: XRD pattern of Mo_5SiB_2-15% TiB_2 material obtained by the chemical oven technique and heated to 1000 °C in O_2/Ar flow.

It can be seen that two of the major initial phases, T_2 and TiB_2 remained in the oxidation product. According to the TGA curves, mass gain started at 400 °C. This mass gain was apparently caused by the oxidation of Mo. For this reason, MoB was decomposed into Mo and the boron-silicon compound, $B_{18}Si$. In addition, the products did not have oxides phases at 1000 °C.

Figure 4.3.4.3 shows the XRD pattern of the oxidation products at 1500 °C. It is seen that the oxidation product had the original three phases and did not have any oxides or borosilicate layers. This XRD pattern is in agreement with the DSC curves. Recall, the onset of an endothermic reaction corresponding to melting was at about 1350 °C and its maximum was at about 1450 °C. This reaction is in agreement with the melting of the borosilicate glass found at the oxidation product at 1000 °C. This means, the layer melt and its components disassociated and reacted with the isolated Mo particles to form again MoB phase.

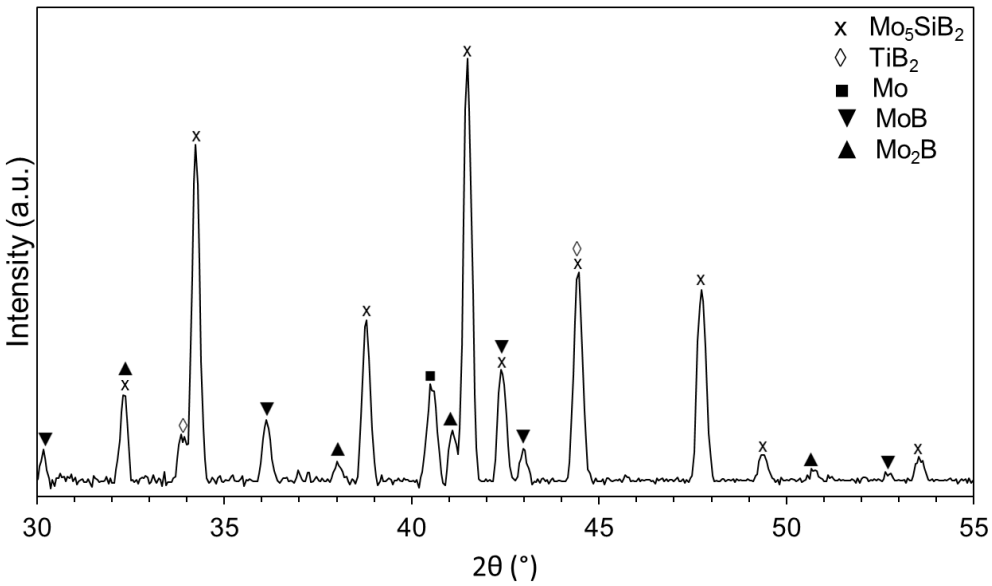

Figure 4.3.4.3: XRD pattern of Mo_5SiB_2–TiB_2 material obtained by the chemical oven technique and heated to 1500 °C in O_2/Ar flow [44].

4.3.5 Elastic modulus and hardness of Mo_5SiB_2-TiB_2 materials fabricated using the chemical oven technique.

The calculated elastic modulus for Mo_5SiB_2-TiB_2 materials was 135 GPa, while the overall hardness was 2.40 GPa. These properties are worse than for Mo-Si-B materials reported in literature. This is apparently associated with the insufficient density and significant porosity of the combustion synthesis products.

4.4 Mo_5SiB_2-TiC materials fabricated by the chemical oven technique

Since the composition corresponding to 15 wt% TiB_2 show promising results during MASHS, the composition tested was the mixture designed for 15 wt% TiC. Also, the same amount of main Mo_5SiB_2 mixture should be used for characterization and comparison with its TiB_2 counterpart.

As expected, the combustion was fast and violent. In addition, the total energy from the booster shell was enough to fully burn the core pellet. In Figure 4.4.1 is seen that the product is shiny and has a metallic appearance. Also, pores and cracks are visible on the product surface.

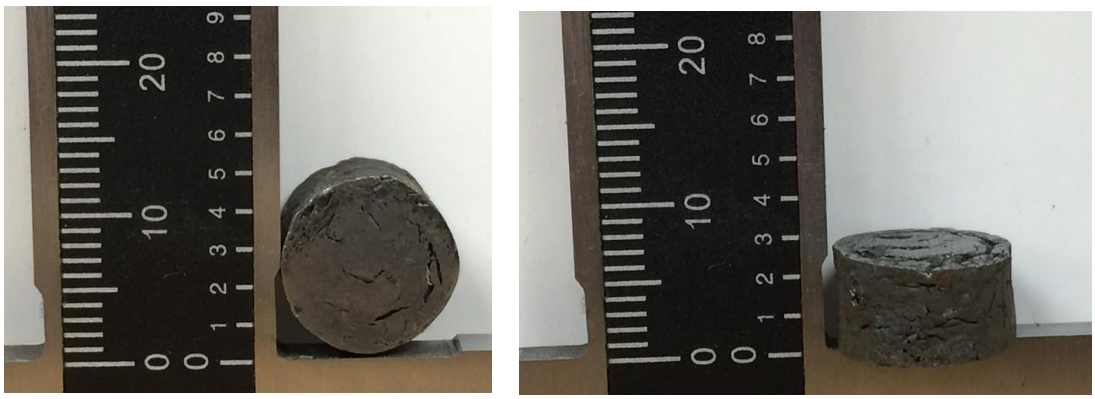

Figure 4.4.1: Combustion products of Mo/Si/B/Ti/C mixture designed for 85% Mo_5SiB_2 and 15% TiC obtained by the chemical oven technique.

With an actual density of 5.26 g/cm^3, the relative density of this material is 73%. Since there is no data for the density of Mo_5SiB_2-TiC materials, it can only be compared with the TiB_2 materials. The chemical oven technique improved the density of the products by 30%.

4.4.1 X-ray diffraction analysis of Mo_5SiB_2-TiC materials fabricated by the chemical oven technique

Materials based on Mo_5SiB_2-TiC with a mixture designed for 15 wt% TiC were characterized using X-ray diffraction analysis. It is seen in Figure 4.4.1.1 that Mo_5SiB_2, TiB_2, and MoB phases were found in the combustion products. In addition, the other desired phase, TiC, was accompanied by Mo_2B. As a consequence, MoB peaks are smaller than the ones found in the Mo_5SiB_2-TiB_2 materials.

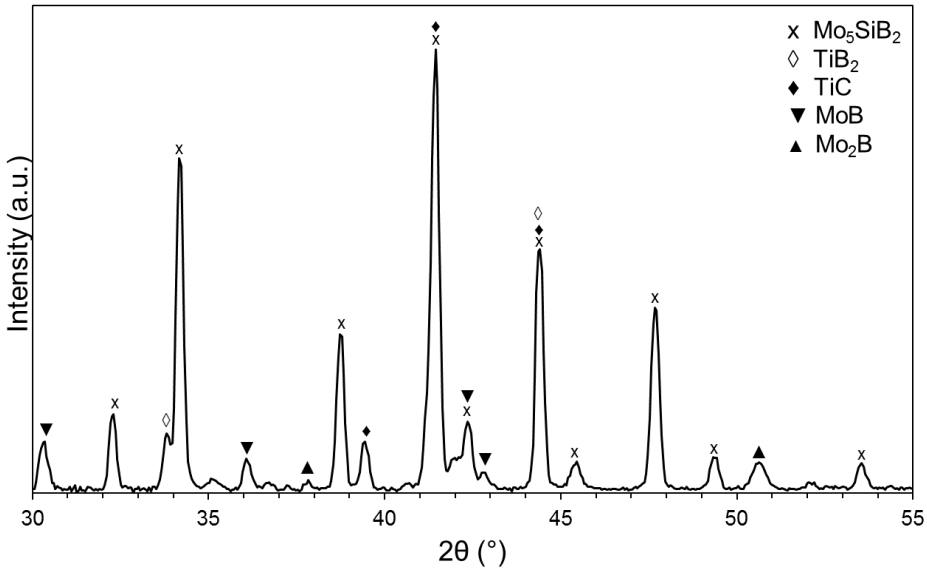

Figure 4.4.1.1: XRD pattern of products obtained by combustion (chemical oven) of Mo/Si/B/Ti/C mixture designed for 85% Mo5SiB2 and 15% TiC [44].

4.4.2 Thermogravimetric analysis of Mo_5SiB_2-TiC materials fabricated using the chemical oven technique

Four samples of Mo_5SiB_2-TiC materials with a composition of 15 wt% TiC, obtained with the chemical oven technique, were tested for oxidation using the thermogravimetric analysis. Figure 4.4.2.1 shows the oxidation behavior of these samples.

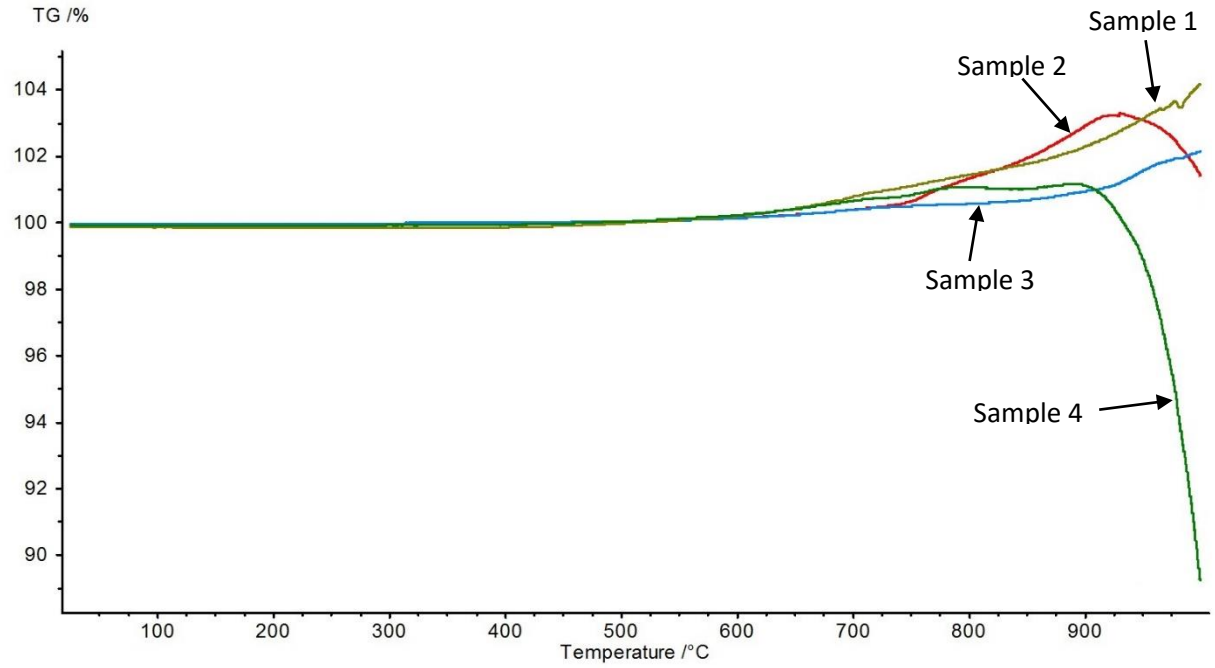

Figure 4.4.2.1: Thermogravimetric curves for samples fabricated by the chemical oven technique with mixture designed 85% Mo_5SiB_2 and 15% TiC.

In all cases, the mass gain started at around 600 °C. However, not all samples behaved similarly. Samples 2 and 4 exhibited a larger mass gain than samples 1 and 3. Also, samples 2 and 4 experienced mass loss at around 930 °C and 900 °C, respectively. Sample 4 experienced a 12% mass loss, being the sample with the highest loss. On the other hand, samples 1 and 3 experienced a quasi-linear oxidation rate and exhibited relatively small mass gains of 4% and 2%, respectively.

4.4.3 Differential scanning calorimeter analysis of Mo_5SiB_2-TiC materials fabricated using the chemical oven technique

Four samples of Mo_5SiB_2-TiC materials with a composition of 15 wt% TiC, obtained with the chemical oven technique, were tested for oxidation using differential scanning calorimeter. Figure 4.4.3.1 shows the oxidation behavior of these samples at temperatures up to 1500 °C.

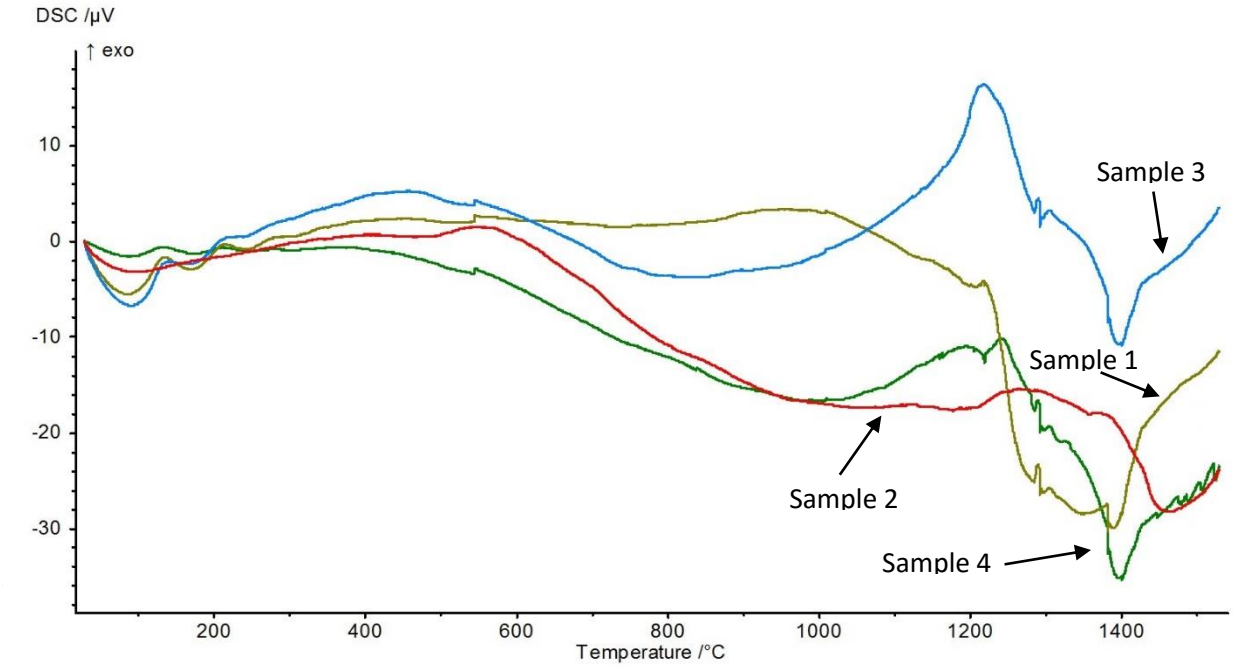

to melt at a temperature as low as 650 °C. Then, there is a second exothermic peak at about 1250 °C that is followed by an endothermic peak with a maximum at about 1450 °C.

Sample 3 started to melt at relatively low temperatures. It displayed an endothermic peak with its onset at about 600 °C and maximum at approximately 850 °C. The, the onset of the largest exothermic peak is at 1000 °C. Again, this is in agreement with the TG curves that showed a small mass gain at that temperature. The maximum of this peak is at 1200 °C. But, it is followed by a very distinct endothermic peak with its maximum at 1400 °C.

Finally, sample 4 behaved similar to sample 3. It showed an endothermic peak with a maximum at 450 °C.

This means that at temperatures above 1200 °C, Mo_5SiB_2-TiC materials fabricated with the chemical oven technique melted.

4.4.4 X-ray diffraction analysis of the oxidation products of Mo_5SiB_2-TiC materials fabricated using the chemical oven technique

The oxidation products at temperatures of 1000 °C and 1500 °C were characterized using X-ray diffraction analysis. Figure 4.4.4.1 shows the typical spectrum of the oxidation products at 1000 °C.

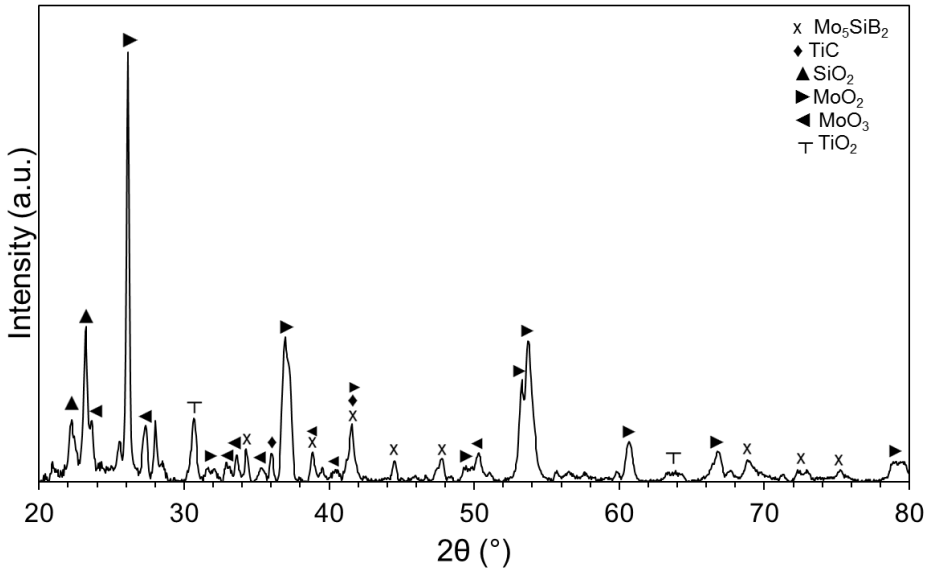

Figure 4.4.4.2: XRD pattern of Mo_5SiB_2-15% TiC material obtained by the chemical oven technique and heated to 1000 °C in O_2/Ar flow.

It is seen that multiple oxide phases were formed at 1000 °C. Phases such as SiO_2, MoO_2, MoO_3, and TiO_2 appeared instead of the missing TiB_2, MoB, and Mo_2B. This means that oxidation occurred at temperatures below 1000 °C and the DSC curves are in agreement with the spectrum. In addition, small peaks of Mo_5SiB_2 and TiC were found, but the major peaks correspond to MoO_2.

Figure 4.4.4.3 shows the XRD pattern of the oxidation products at 1500 °C. It is seen that no oxides were formed at 1500 °C. Also, a molybdenum phase is found in the spectrum presumably for the decomposition of MoO_2 and MoO_3. MoO_3 decomposes at 1100 °C while MoO_3 melts boils at 1155 °C [9]. This is in agreement with the endothermic peak with the onset at around 1100 °C shown in the DSC curves. It cannot be concluded that TiO_2 and SiO_2 were not present at 1500 °C

since their melting points are higher than 1500 °C. One explanation is that these phases were found in relatively small quantities during thermogravimetric analysis and the XRD was not able to properly characterize them.

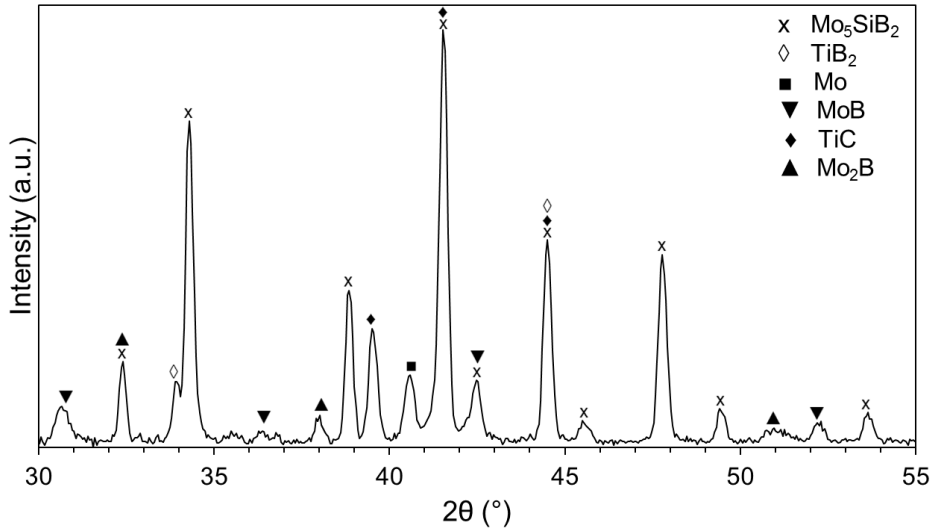

Figure 4.4.4.3: XRD pattern of products obtained by combustion (chemical oven) of Mo/Si/B/Ti/C mixture designed for 85% Mo_5SiB_2 and 15% TiC [44].

4.4.5 Elastic modulus and hardness of Mo_5SiB_2-TiC materials fabricated using the chemical oven technique.

The calculated elastic modulus for Mo_5SiB_2-TiC materials was 109 GPa, while the overall hardness was 1.24 GPa. Again, these properties are worse than for Mo-Si-B materials reported in literature and even lower than for Mo-Si-B-Ti materials presented in this work. Likewise, insufficient density and significant porosity of the combustion synthesis products affect the overall hardness and total elastic modulus.

4.5 Mo-Mo_3Si-Mo_5SiB_2 fabricated by the chemical oven technique

The chemical oven technique has also enabled combustion synthesis of α-Mo-Mo_3Si-Mo_5SiB_2 materials. As in all other chemical oven tests, vigorous combustion of the shell mixture

and complete combustion of the core pellet were observed. Also, the products show the same visible defects on their surface. Figure 4.5.1 shows the combustion product of this material. It is seen that the surface is porous and there are some visible cracks, but the obtained material has a metallic appearance.

Figure 4.5.1: Combustion products of Mo/12Si/8.5B mixture obtained by the chemical oven technique.

The densities of these materials were in the range of 7.0-7.6 g/cm^3. This resulted in a relative density of 80-87%.

4.5.1 X-ray diffraction analysis of α-Mo-Mo_3Si-Mo_5SiB_2 materials fabricated by the chemical oven technique

Figure 4.5.1.1 shows a typical XRD pattern of the material obtained from Mo/12Si/8.5B mixture using the chemical oven technique. The peaks correspond to the desired α-Mo, Mo_5SiB_2, and Mo_3Si phases, with no other phases detected.

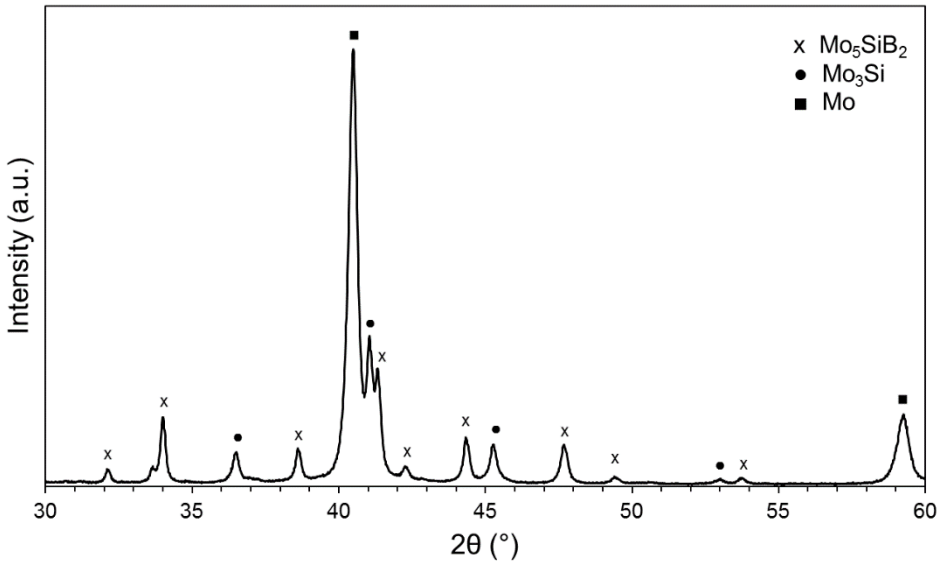

Figure 4.5.1.1: XRD pattern of products obtained by combustion of Mo/12Si/8.5B mixture.

Considering the highest peak for each phase, Mo/Mo_3Si/Mo_5SiB_2 intensity ratio is 3.7: 1.3: 1. Since the highest peaks of the three phases are close to each other and partly overlap, the intensity ratio was estimated based on the peak heights only. Although accurate quantitative analysis of XRD results was not conducted, it is seen that Mo dominates in the XRD pattern and the highest peak of Mo_3Si exceeds the highest peak of Mo_5SiB_2. This is in agreement with the ratio of phase contents in the desired Mo–12Si–8.5B material, where Mo/Mo_3Si/Mo_5SiB_2 mole and mass ratios are 8.23: 1.82: 1 and 9.55: 1.86: 1, respectively (here the densities of the three phases were assumed to be 10.22, 8.97, and 8.81 g/cm^3, respectively [12].

4.5.2 Thermogravimetric analysis of α-Mo-Mo_3Si-Mo_5SiB_2 materials fabricated by the chemical oven technique

Three samples of three-phase materials obtained with the so-called “chemical oven” technique were tested using thermogravimetric analysis. Figure 4.5.2.1 shows the TG curves for this oxidation test.

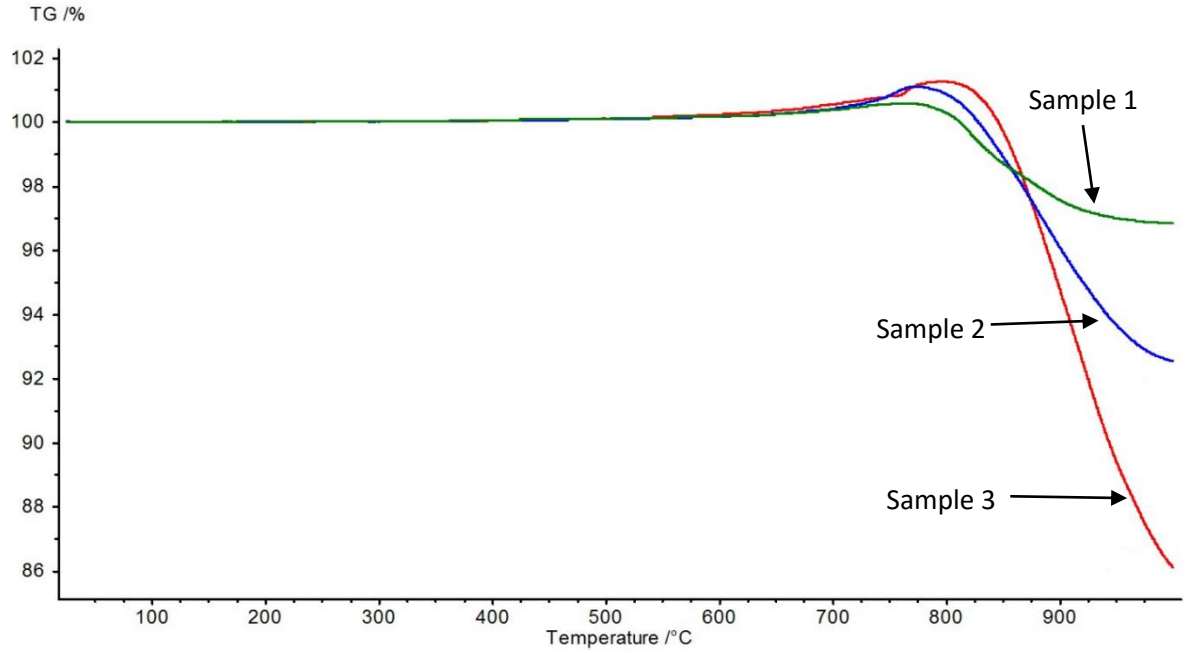

Figure 4.5.2.1: Thermogravimetric curves for samples fabricated by the chemical oven technique of mixture Mo/12Si/8.5B.

It is seen that the three samples behaved similarly, though with different rates of the mass change. Sample 1 experienced a mass gain of about 0.5% at 700 °C. Then, it was followed by a sudden mass loss at 800 °C and reached a maximum loss of 2% at 1000 °C.

Likewise, sample 2 exhibited a mass gain of 1% at about 700 °C. Mass loss started at 800 °C and reached a maximum mass loss of 8% at 1000 °C.

Sample 3 has the lowest oxidation resistance. The oxidation started at 700 °C and reached a maximum mass gain of about 1.5%. Then, a sudden mass loss at 800 °C caused the sample to experience a 15% mass loss.

4.5.3 Compression strength of α-Mo-Mo_3Si-Mo_5SiB_2 materials fabricated by the chemical oven technique

The compressive strength of Mo−12Si−8.5B alloy synthesized by the chemical oven technique was as high as 524 MPa, while the density was in the range of 7.0−7.6 g/cm^3. Note that molybdenum possesses a compressive strength of 400 MPa [38] and has a density of 10.2 g/cm^3, i.e. the obtained materials are stronger and lighter than molybdenum. To our knowledge, there are no data on compressive strength of Mo−12Si−8.5B alloys prepared by arc melting in the literature, but it has been reported that these materials have a flexural strength of 539 MPa at room temperature [7]. Apparently, Mo-12Si-8.5B materials obtained by chemical oven and arc melting have a similar strength.

Chapter 5: Conclusion

The desire to increase the efficiency of gas-turbine power plants has ignited the search for new structural materials that can operate at higher temperatures, without the need for cooling, than the present Ni-based superalloys. Investigations have been made and new materials have been created with the use of complex and expensive techniques. In many cases, these techniques required long processing times that can affect the quality of the end products. However, this study has presented both an attractive technique alternative and new materials for ultrahigh-temperature applications.

It has been shown that Mo_5SiB_2-based materials have been fabricated by mechanical activated self-propagating high temperature synthesis (MASHS). Mo_5SiB_2-TiB_2, Mo_5SiB_2-TiC, and α-Mo/Mo_3Si/Mo_5SiB_2 materials were investigated using this technique. It was shown that MASHS did not reach the melting temperatures of any of the reactants and the combustion was driven by solid-phase diffusion. For this reason, the relative density of the end products was as low as 50%. Consequently, the oxidation resistance of these materials was poor. In addition, it was shown that it was not possible to obtain materials without unwanted phases using conventional SHS due to the low combustion temperatures. In addition, mixtures designed to obtain Mo_5SiB_2-TiC phases were unable to ignite using MASHS.

SHS has major limitations which are the dependence on the mixture exothermicity and the inevitable heat losses. For this reason, another combustion synthesis technique was applied. The so-called “chemical oven” technique successfully achieved a combustion temperature higher than the melting points of the reactants without the need for additional energy input. All mixture compositions were able to burn successfully and their relative densities were as high as 87% . In addition, less unwanted phases were found in both Mo_5SiB_2-TiB_2 and Mo_5SiB_2-TiC materials while α-Mo/Mo_3Si/Mo_5SiB_2 materials did not contain any parasitic phases. However, the “chemical oven” technique delivered cracked products because of the violent combustion process.

This is a major limitation for this technique, but it can be overshadowed by the simplicity of the process and the purity of the end products.

From the materials studied in this manuscript, Mo_5SiB_2-TiB_2 materials obtained by the chemical oven technique delivered the best oxidation resistance and mechanical properties. These characteristics were 135 GPa for the elastic modulus and 2.40 GPa for the overall hardness of 2.40 GPa. Likewise, Mo_5SiB_2-TiC materials had an elastic modulus of 109 GPa of and an overall hardness of 1.24 GPa. In addition, α-Mo/Mo_3Si/Mo_5SiB_2 materials exhibited the worse oxidation resistance, though they had a compression strength of 400 MPa. Yet, for all materials, these properties are worse than for Mo-Si-B materials reported in the literature. This means that the so-called "chemical oven" technique has certain limitations that hinder the quality of the end products even though the materials obtained by this technique are denser than the products of conventional SHS.

It is important to note that there is still much to be done to achieve the desired 100% relative density. However, this technique is an attractive alternative to conventional methods owing to the fact that its minimum energy required and short fabrication process enable the synthesis of materials with comparable characteristics, or at least, the phases obtained were the same as in the products fabricated with other, time- and energy-consuming methods.

References

[1] N. P. Padture, M. Gell and E. H. Jordan, "Thermal barrier coatings for gas-turbine engine applications," *Science,* vol. 296, pp. 280-284, 2002.

[2] Z. Yao, J. J. Stiglich and T. S. Sudarshan, "Molybdenum silicide based materials and their properties," *Journal of Materials Engineering and Performance,* vol. 8, no. 3, pp. 291-304, 1999.

[3] J. J. Petrovic, "Mechanical behavior of $MoSi_2$ and $MoSi_2$ composites," *Materials Science and Engineering,* vol. A192, pp. 31-37, 1995.

[4] A. K. Vasudevan and J. J. Petrovic, "A comparative overview of molybdenum disilicide composites," *Materials Science and Engineering,* vol. A 155, pp. 1-17, 1992.

[5] R. Gibala, A. K. Ghosh, D. C. Van Aken, D. J. Srolovitz, A. Basu, H. Chang, D. P. Mason and W. Yang, "Mechanical behavior and interface design of $MoSi_2$-based alloys and composites," *Materials Science and Engineering,* vol. A 155, no. 1992, pp. 147-158, 1992.

[6] K. Sadananda, C. R. Feng, R. Mitra and S. C. Deevi, "Creep and fatigue properties of high temperature silicides and their composites," *Materials Science and Engineering,* vol. A261, pp. 223-238, 1999.

[7] R. B. Schwarz, S. R. Srinivasan, J. J. Petrovic and C. J. Maggiore, "Synthesis of molybdenum disilicide by mechanical alloying," *Materials Science and Engineering,* vol. A155, pp. 75-83, 1992.

[8] F. Chu, D. J. Thoma, K. J. McClellan, P. Peralta, F. X. Li and E. Fodran, "Processing and properties of Mo_5Si_3 single crystals and alloys," in *MRS Fall Meeting,* 1998.

[9] J. A. Lemberg and R. O. Ritchie, "Mo-Si-B alloys for ultrahigh-temperature structural applications," *Advanced Materials,* vol. 24, pp. 3445-34480, 2012.

[10] R. Mitra, "Mechanical behavior and oxidation resistance of structural silicides," *International Materials Reviews,* vol. 51, pp. 13-60, 2006.

[11] M. Akinc, M. K. Meyer, M. J. Kramer, A. J. Thom, J. J. Huebsch and B. Cook, "Boron-doped molybdenum silicides for structural applications," *Materials Science and Engineering,* vol. A261, pp. 13-23, 1999.

[12] J. Schneibel, M. Kramer, O. Unal and R. Wright, "Processing and mechanical properties of a molybdenum silicide with the composition Mo-12Si-8.5B," *Intermetallics,* vol. 9, pp. 25-31, 2001.

[13] H. Choe, D. Chen, J. Schneibel and R. Ritchie, "Ambient to high temperature fracture toughness and fatigue-crack propagation behavior in a Mo-12Si-8.5B," *Intermetallics,* vol. 9, pp. 319-329, 2001.

[14] M. Kruger, S. Franz, H. Saage, M. Heilmaier, J. Schneibel, P. Jehanno, M. Boning and H. Kestler, "Mechanically alloyed Mo-Si-B alloys with a continuous a-Mo matrix and improved mehcanical properties," *Intermetallics,* vol. 16, pp. 933-941, 2008.

[15] J. Shackelford and W. Alexander, CRC Materials Science and Engineering Handbook, Boca Raton: CRC Press, 2000.

[16] S. Miyamoto, K. Yoshimi, S.-H. Ha, T. Kaneko, J. Nakamura, T. Sato, K. Maruyama, R. Tu and T. Goto, "Phase equilibria, microstructure, and high-temperature strength of TiC-added Mo-Si-B alloys," *Metallurgical and Materials Transactions,* vol. 45A, pp. 1112-1123, 2014.

[17] K. Yoshimi, J. Nakamura, D. Kanekon, S. Yamamoto, K. Maruyama, H. Katsui and T. Goto, "High-temperature compressive properties of TiC-added Mo-Si-B alloys," *JOM,* vol. 66, no. 9, pp. 1930-1938, 2014.

[18] H. Ledbetter and T. Tanaka, "Elastic-Stiffness coefficients of titanium diboride," *Journal of Research of the National Instittute of Standards and Technology,* vol. 114, pp. 333-339, 2009.

[19] A. Yamauchi, K. Yoshimi, K. Kurokawa and S. Hanada, "Synthesis of Mo-Si-B in situ composites by mechanical alloying," *Journal of Alloys and Compounds,* Vols. 434-435, pp. 420-423, 2007.

[20] A. Merzhanov and I. Borovinskaya, "Historical retrospective of SHS: An Autoreview," *International Journal of Self-Propagating High-Temperature Synthesis,* vol. 17, pp. 242-265, 2008.

[21] C. Gras, E. Gaffet and F. Bernard, "Combustion wave structure during the $MoSi_2$ synthesis by mechanically-activated self-propagating high-temperature synthesis (MASHS): In situ time-resolved investigations," *Intermetallics,* vol. 14, pp. 521-529, 2006.

[22] M. A. Korchagin and D. V. Dudina, "Application of self-propagating high-temperature synthesis and mechanical activation for obtaining nanocomposites," *Combustion, Explosion, and Shock Waves,* vol. 43, pp. 176-187, 2007.

[23] E. A. Levashov, Y. S. Pogozhev, Y. A. Potanin, N. A. Kochetov, Y. D. Kovalev, N. V. Shvyndina and T. A. Sviridova, "Self-propagating high-temperature synthesis of advanced ceramics in the Mo-Si-B system: Kinetics and mechanism of combustion and structure formation," *Ceramics International,* vol. 40, pp. 6541-6552, 2014.

[24] J. J. Petrovic and A. K. Vasudevan, "Key developments in high temperature structural silicides," *Materials science and Engineering,* vol. 261, pp. 1-5, 1999.

[25] M. K. Meyer and M. Akinc, "Isothermal oxidation behavior of Mo-Si-B intermetallics at 1450 °C," *Journal of the American Ceramic Society,* vol. 79, no. 10, pp. 2763-2766, 1996.

[26] M. Meyer, A. Thom and M. Akinc, "Oxide scale formation and isothermal oxidation behavior of Mo-Si-B intermetallics at 600-1000 C," *Intermetallics,* vol. 7, pp. 153-162, 1999.

[27] M. Akinc, M. K. Meyer, M. J. Kramer, A. J. Thom, J. J. Huebsch and B. Cook, "Boron-doped molybdenum silicides for structural applications," *Materials Science and Engineering,* vol. 261, no. 1-2, pp. 16-23, 1999.

[28] K. Ito, T. Hayashi, M. Yokobayashi, T. Murakami and H. Numakura, "Oxidation protective silicide coating on Mo-Si-B alloys," *Metallurgical and Material Transactions,* vol. 36A, pp. 627-636, 2005.

[29] M. Kruger, P. Jain, K. Kumar and M. Heilmaier, "Correlation between microstructure and properties of fine grained Mo-Mo_3Si-Mo_5SiB_2 alloys," *Intermetallics,* vol. 48, pp. 10-18, 2014.

[30] H. Choe, J. Schneibel and R. Ritchie, "On the fracture and fatigue properties of Mo-Mo_3Si-Mo_5SiB_2 refractory intermetallic alloys at ambient to elevated temperatures (25 C to 1300 C)," *Metallurgical and Materials Transactions A,* vol. 34A, pp. 225-239, 2003.

[31] M. Mendiratta, T. Parthasarathy and D. Dimiduk, "Oxidation behavior of α-Mo-Mo_3Si-Mo_5SiB_2 (T_2) three phase system," *Intermetallics,* vol. 10, pp. 225-232, 2002.

[32] J. Schneibel, C. Liu, D. Easton and C. Carmichael, "Microstructure and mechanical properties of Mo-Mo_3Si-Mo_5SiB_2 silicides," *Materials Science & Engineering A,* vol. 261, pp. 78-83, 1999.

[33] P. Mandal, A. J. Thom, M. J. Kramer, V. Behrani and M. Akinc, "Oxidation behavior of Mo-Si-B alloys in wet air," *Materials Science & Engineering A,* vol. 371, pp. 335-342, 2004.

[34] F. Wang, A.-d. Shan, X.-p. Dong and J.-s. Wu, "Oxidation behavior of multiphase Mo_5SiB_2 (T_2)-based alloys at high temperatures," *Transactions of Nonferrous Metals Society of China,* vol. 17, pp. 1242-1247, 2007.

[35] K. Yoshimi, S. Nakatani, T. Suda, S. Hanada and H. Habazaki, "Oxidation behavior of Mo_5SiB_2-based alloy at elevated temperatures," *Intermetallics,* vol. 10, pp. 407-414, 2002.

[36] D. M. Dimiduk and J. H. Perepezko, "Mo-Si-B alloys: Developing a revolutionary turbine-engine material," *MRS Bulletin*, pp. 639-645, 2003.

[37] A. Alur, N. Chollacoop and K. Kumar, "High-temperature compression behavior of Mo-Si-B alloys," *Acta Materialia*, vol. 52, pp. 5571-5587, 2004.

[38] B. Li, G.-j. Zhang, F. Jiang, S. Ren, G. Liu and J. Sun, "Preparation of fine-grained Mo-12Si-8.5B alloys with improved mechanical properties via a mechanical alloying process," *Journal of Alloys and Compounds,* vol. 609, pp. 80-85, 2014.

[39] P. G. Biragoni and M. Heilmaier, "FEM-simulation of real and artificial microstrcutures of Mo-Si-B alloys for elastic properties and comparison with analytical methods," *Advanced Engineering Materials,* vol. 9, no. 10, pp. 882-887, 2007.

[40] J. J. Kruzic, J. H. Schneibel and R. O. Ritchie, "Fracture and fatigue resistance of Mo-Si-B alloys for ultrahigh-temperature structural applications," *Acta Materialia,* vol. 50, pp. 59-464, 2003.

[41] J. Kruzic, J. Schneibel and R. Ritchie, "Fracture and fatigue resistance of Mo-Si-B alloys for ultrahigh-temperature structural applications," *Scripta Materialia,* vol. 50, pp. 459-464, 2004.

[42] K. Ilhara, K. Ito, K. Tanaka and M. Yamaguchi, "Mechanical properties of Mo_5SiB_2 single crystals," *Materials Science and Engineering,* Vols. 329-331, pp. 222-227, 2002.

[43] K. Ito, K. Ilhara, K. Tanaka, M. Fujikura and M. Yamaguchi, "Physical and mechanical properties of single crystals of the T_2 phase in the Mo-Si-B system," *Intermetallics,* vol. 9, pp. 591-602, 2001.

[44] A. A. Esparza and E. Shafirovich, "Mechanically activated combustion synthesis of molybdenum borosilicides for ultrahigh-temperature structural applications," *Journal of Alloys and Compounds,* vol. 670, pp. 297-305, 2016.

[45] J. Subrahmanyam and M. Vijayakumar, "Review self-propagating high-temperature synthesis," *Journal of Materials Science,* vol. 27, pp. 6249-6273, 1992.

Vita

Alan Alberto Esparza Hernandez was born in Ciudad Juárez, México in 1992. He is the son of Telesforo Esparza and Blanca Hernandez. Alan attended ITESM High School in Ciudad Juárez. He enrolled at University of Texas at El Paso in the Fall of 2010. Alan earned his Bachelor of Science in Mechanical Engineering, graduating Magna Cum Laude in the Spring of 2014. During 2013-2014 academic year, Alan was supported by the Campus Office of Undergraduate Research Initiatives (COURI) to work under the supervision of Dr. Norman D. Love for the project "Air cooled condensers and the application of metal foam on the condensers tubes." He presented his work in April, 2014 at the "2014 COURI Symposium" as well as at the 4th Southwest Energy Science and Engineering Symposium in El Paso. After graduation, he immediately started his M.S. studies at UTEP and joined Dr. Evgeny Shafirovich's research team in the Center for Space Exploration Technology Research. There, he worked for the DOE-sponsored project on mechanically activated synthesis of molybdenum borosilicides. Alan presented his work at the 9th US National Combustion Synthesis in May 2015 as well as at the 5th Southwest Energy Science and Engineering Symposium. A full-length article, titled "Mechanically Activated Combustion Synthesis of Molybdenum Borosilicides for Ultrahigh-Temperature Structural Applications" has been published in the peer-reviewed journal *Journal of Alloys and Compounds* (available online since February 2016 and it will appear in volume 670 in June 2016).

Contact Information: aaesparza3@miners.utep.edu

This thesis was typed by Alan A. Esparza Hernández.